Theoretical Studies on Nonlinear Optical Properties of Formaldehyde Oligomers by *Ab Initio* and Density Functional Theory Methods

HUI-YIN WU,[1] AJAY CHAUDHARI,[1,2] SHYI-LONG LEE[1]

[1]*Department of Chemistry and Biochemistry, National Chung-Cheng University, Ming-Hsiung, Chia-Y I, Taiwan-621*

[2]*Department of Physics, Pennsylvania State University, 104 Davey Lab., University Park, Pennsylvania 16801*

Received 18 December 2004; Accepted 14 April 2005
DOI 10.1002/jcc.20294
Published online in Wiley InterScience (www.interscience.wiley.com).

Abstract: The first and second hyperpolarizability β and γ are obtained for formaldehyde oligomers $(H_2CO)_n$ (n = 1–7) using computational methods. We have used the finite field (FF) approach and hyperpolarizability density analysis (HDA) to predict the microscopic first and second nonlinear hyperpolarizability of the formaldehyde oligomers. The spatial contributions of electrons to the hyperpolarizability by using plots of HDA are presented. It has been found from the numerical stability checking of the hyperpolarizability calculations that the calculated values by FF method are more stable than those by HDA approach. The values of β are zero when n is even as the molecule possesses centrosymmetry, and when n is odd, the differences among β values are not clear. The γ values are increased with increase in n.

© 2005 Wiley Periodicals, Inc. J Comput Chem 26: 1543–1564, 2005

Key words: formaldehyde oligomers; nonlinear optical properties; finite field method; hyperpolarizability density analysis

Introduction

Today, organic molecular materials become new nonlinear optical materials for potential applications owing to several advantages, such as the possibility of high NLO response and high optical damage resistance. Varieties of phenomena of nonlinear optics can be induced by a strong, powerful electromagnetic field like that of a laser beam. The properties of such materials can be expressed in terms of molecular properties, the molecular packing in the bulk, and intermolecular interactions.[1–5]

The formaldehyde molecule, H_2CO, is a parent compound for many species.[6] Today, it is widely used in industry. More than half is used to make plastics and adhesive resins used in the manufacture of fiberboard, plywood, and particleboard. It also has important applications in textiles, the oil industry, the automotive industry, and household products.

Although formaldehyde has been the subject of both quantum chemical and experimental studies,[7–29] there is still interest in the structure–property relationships for this model species. The structures and vibrational frequencies of a formaldehyde monomer have been analyzed by numerous theoretical[14–22] and experimental[23–26] work. Theoretical studies were based on the *ab initio* Hartree–Fock (HF) theory[12,15–17] and Møller–Plesset second-order perturbation (MP2) theory.[13,14,16–19] The purpose of the present article is to do a systematic theoretical study of the structure and nonlinear optical properties of the formaldehyde oligomers, $(H_2CO)_n$ (n = 1–7). We first compare both the molecular geometries and the harmonic wave numbers of the monomeric H_2CO molecule with experimental and calculated data. We then calculate the geometrical parameters of oligomeric structures. The optimized structures of formaldehyde oligomers are used to gain the NLO properties. We do not attempt to obtain the absolute values for hyperpolarizabilities. Instead, our attention is focused on the qualitative features and semiquantitative trend of our results on β and γ for the formaldehyde oligomers. Some *ab initio* calculational results on formaldehyde have already been reported in the literature.[12–22] These studies provided some useful geometric data for comparison, but they are not related with the study of nonlinear optical properties. The present article is organized as follows. In the next section we

Correspondence to: A. Chaudhari, e-mail: ajaychau5@yahoo.com; S.-L. Lee, e-mail: chesll@ccu.edu.tw

Present address: 104 Davey Lab, Department of Physics, Pennsylvania State University, University Park, PA 16802.

Contract/grant sponsor: National Science Council, Taiwan

© 2005 Wiley Periodicals, Inc.

briefly interpret the quantum chemical calculations. Then, the results of formaldehyde oligomers are discussed in connection with the structure–property correlation. This is followed by a conclusion.

Computational Details

In this work, all the computations have been performed by Gaussian 98 program package.[30] HF, MP2, DFT (BLYP and B3LYP) methods have been used with different basis sets.

Hyperpolarizability Calculations

For various molecule–molecule interactions, hyperpolarizability is a useful measure. The methods by Nakano et al.[31–42] are adopted for analyzing the static hyperpolarizability computed by the finite-field approach. Polarizability and hyperpolarizability can be regarded as the factors related to the first- and higher order derivative of the electrons density. These quantities are expected to be helpful for investigating the stability of chemical bonds and characteristics of intermolecular interactions.

Finite-Field Method

We confine our attention to the main components of β and γ, that is, β_{zzz} and γ_{zzzz}, for the model systems, because the relations among β_{zzz} and γ_{zzzz} with polarization in the direction are primarily considered in this work. The β_{zzz} and γ_{zzzz} are calculated by the numerical differentiation of the total energy E with respect to the applied field by, for example, the FF method suggested by Yamada et al.[33,34]

$$\beta_{zzz} = \{-E(2F_z) + E(-2F_z) + 2[E(F_z) - E(-F_z)]\}/4(F_Z)^3 \quad (1)$$

$$\gamma_{zzzz} = \left\{ \begin{matrix} E(3F_z) - 12E(2F_z) + 39E(F_z) - 56E(0) \\ + 39E(-F_z) - 12E(-2F_z) + E(-3F_z) \end{matrix} \right\}/36(F_Z)^4 \quad (2)$$

Here, $E(F_z)$ indicates the total energy in the presence of the field F applied in the z direction.

We use several minimum field strengths to avoid numerical errors. After the numerical differentiation using these fields, we adopt the numerically stable range for computing β_{zzz} and γ_{zzzz}.

Hyperpolarizability Density Analysis

We adopt Hyperpolarizability density analysis[33–43] for analyzing the static hyperpolarizability in the finite-field approach by using the derivatives of charge densities with respect to the applied fields. This method is shown to be useful for obtaining pictorial and intuitive understanding of the spatial characteristics of the static hyperpolarizability. The box size ($79 \times 79 \times 81 = 518{,}003$ pts) is similar for all the oligomers studied here $(HCHO)_n$, $n = 1$–7, where a grid size is proportional to n (for $n = 1$, grid size = 0.088881, $n = 2$, grid size = 0.106152, etc.).

The charge density function $\rho(r, F)$ is expanded in powers of the field F as

$$\rho(r, F) = \rho^{(0)}(r) + \sum_j \rho_j^{(1)}(r) F_j + \frac{1}{2!} \sum_j \sum_k \rho_{jk}^{(2)}(r) F_j F_k + \frac{1}{3!} \sum_j \sum_k \sum_l \rho_{jkl}^{(3)} F_j F_k F_l + \ldots . \quad (3)$$

From this equation and the expansion formula of the dipole moment in powers of the field, the static β and γ can be expressed by

$$\beta_{ijk} = -\frac{1}{2!} \int r_i \rho_{jk}^{(2)}(r) dr^3 \quad (4)$$

$$\gamma_{ijkl} = -\frac{1}{3!} \int r_i \rho_{jkl}^{(3)}(r) dr^3 \quad (5)$$

where

$$\rho_{jk}^{(2)} = \left. \frac{\partial^2 \rho}{\partial F_j \partial F_k} \right|_{F=0} \quad (6)$$

$$\rho_{jkl}^{(3)} = \left. \frac{\partial^3 \rho}{\partial F_j \partial F_k \partial F_l} \right|_{F=0} \quad (7)$$

The second- and third-order derivative of the electron densities with respect to the applied electric fields are referred to as the β and γ density, respectively. We also limit our attention to the β and γ densities [$\rho_{zz}^{(2)}(r)$ and $\rho_{zzz}^{(3)}(r)$] corresponding to the β_{zzz} and γ_{zzzz}, and they are calculated at each spatial point in the discretized space by using the following second- and third-order numerical differentiation formula.

$$\rho_{zz}^{(2)}(r) = \{\rho(r, F_z) + \rho(r, -F_z) - 2\rho(r, 0)\}/(F_Z)^2 \quad (8)$$

$$\rho_{zzz}^{(3)}(r) = \{\rho(r, 2F_z) - \rho(r, -2F_z) - 2[\rho(r, F_z) - \rho(r, -F_z)]\}/2(F_Z)^3 \quad (9)$$

where $\rho(r, F_z)$ represents the charge density at a spatial point r in the presence of the field F_z.

We are working on density plots using a five-point formula for second-order differentiation and a six-point formula for third-order differentiation.

Result and Discussions

Geometries

Monomer

In this section formaldehyde monomer has been analyzed by calculations using different theoretical methods, including HF,

Table 1. Computed and Experimental Geometries along with Dipole Moment (Debye) for H_2CO.

Method	Bond lengths, Å basis set	Bond angles, deg				Energy (a.u.) SCF	μ
		C—O	C—H	∠HCH	∠HCO		
BLYP	6-31G	1.243	1.113	115.2	122.3	−114.4373178	2.27
	6-31G(*d*)	1.218	1.120	115.1	122.4	−114.4721979	2.03
	6-31+G(*d*)	1.221	1.118	116.0	121.9	−114.4823573	2.40
	6-31+G(*d*,*p*)	1.221	1.118	116.0	121.9	−114.4849382	2.40
	6-31+G(2*d*,*p*)	1.215	1.118	116.1	121.9	−114.4906315	2.34
	6-311G(3*df*,2*p*)	1.208	1.116	115.6	122.1	−114.5191029	2.07
B3LYP	6-31G	1.231	1.102	115.6	122.1	−114.4611366	2.47
	6-31G(*d*)	1.206	1.110	115.2	122.3	−114.5004726	2.19
	6-31+G(*d*)	1.209	1.108	116.2	121.8	−114.5088406	2.52
	6-31+G(*d*,*p*)	1.209	1.108	116.2	121.8	−114.5115243	2.52
	6-31+G(2*d*,*p*)	1.203	1.108	116.3	121.8	−114.5172040	2.44
	6-311G(3*df*,2*p*)	1.196	1.106	115.9	122.0	−114.5456435	2.20
Experiment	[a]	1.208	1.116	116.5			2.32[c]
	[b]	1.203	1.100	116.1			2.33[d]

[a]Ref. 29.
[b]Ref. 23.
[c]Ref. 27.
[d]Ref. 28.

MP2, BLYP, and B3LYP. We also investigate the basis set effects by using the split-valence and extended basis sets augmented by diffuse and polarization functions. Comparing various methods with the same basis set, it has been observed that the molecular parameters from the DFT calculations agree better with the experimental data than those from other calculations except HF values. Therefore, only the geometrical parameters obtained using DFT methods are reported in this article. Table 1 collects the ground-state equilibrium geometries, electronic energies, and dipole moment for the formaldehyde monomer using DFT methods along with available experimental data. We can observe that the value for BLYP/6-31+G(2*d*,*p*) is closer to the experimental data.

The calculated and experimental vibrational frequencies of formaldehyde monomer are given in Table 2. The positions of

Table 2. Harmonic Vibrational Frequencies (cm^{-1}) for H_2CO.

Method	Basis set	Vibrational frequencies					
		ω1 (A1)	ω2 (B2)	ω3 (A1)	ω4 (B2)	ω5 (B1)	ω6 (A1)
BLYP	6-31G	1683.6	2905.2	1512.7	1235.8	1159.8	2849.5
	6-31G(*d*)	1773.8	2847.8	1520.7	1241.9	1151.9	2811.3
	6-31+G(*d*)	1744.8	2867.4	1501.4	1228.3	1144.8	2821.7
	6-31+G(*d*,*p*)	1740.6	2862.2	1494.7	1223.8	1147.8	2810.3
	6-31+G(2*d*,*p*)	1739.8	2844.4	1488.6	1222.7	1144.5	2797.5
	6-311G(3*df*,2*p*)	1759.5	2806.2	1495.0	1231.9	1155.7	2771.2
B3LYP	6-31G	1748.0	3034.9	1560.2	1273.7	1203.1	2963.7
	6-31G(*d*)	1849.5	2968.1	1563.0	1279.6	1198.4	2917.0
	6-31+G(*d*)	1823.0	2990.1	1544.7	1267.3	1191.2	2930.9
	6-31+G(*d*,*p*)	1819.5	2979.1	1537.1	1262.1	1193.8	2914.3
	6-31+G(2*d*,*p*)	1817.7	2958.1	1530.4	1261.2	1190.7	2897.9
	6-311G(3*df*,2*p*)	1834.5	2925.0	1535.1	1269.6	1200.5	2874.2
exp	[a]	1764	3009	1563	1287	1191	2944
	[b]	1777.8	3012.0	1544.0	1269.4	1188.3	2937.4
	[c]	1746	2843	1500	1249	1167	2783

[a]Experimental harmonized wave numbers of fundamentals mode from ref. 24.
[b]Experimental harmonized wave numbers of fundamentals mode from ref. 25.
[c]Wave numbers of fundamental modes from ref. 26.

Table 3. Computed Geometries and Wave Number (cm^{-1}) for C═O Stretching Vibration for Formaldehyde Dimer.

		Bond lengths, Å			Bond angles, deg				
	Basis set	C—O	C—H		O · · · H	∠HCH	∠HCO		Energy (a.u.)
BLYP	6-31G	1.248	1.107[a]	1.113[b]	2.47[c]	116.9	121.5[d]	121.4[e]	−228.8815770
	6-31+G(*d*)	1.225	1.114	1.118	2.67	117.0	121.6	121.3	−228.9678422
	6-31+G(2*d*,*p*)	1.219	1.114	1.118	2.65	117.1	121.5	121.3	−228.9843354
B3LYP	6-31G	1.236	1.097	1.102	2.43	117.2	121.4	121.3	−228.9300438
	6-31+G(*d*)	1.213	1.104	1.108	2.58	117.2	121.5	121.2	−229.0218174
	6-31+G(*d*,*p*)	1.213	1.104	1.108	2.55	117.3	121.4	121.2	−229.0273539
	6-31+G(2*d*,*p*)	1.207	1.105	1.109	2.57	117.3	121.4	121.2	−229.0384460

		Wave number for the C═O stretching vibration of dimer		
		Dimer	Monomer	Exp.
BLYP	6-31G	1664.6	1683.6	1764[f]
	6-31+G(*d*)	1734.2	1744.8	1777.8[g]
	6-31+G(2*d*,*p*)	1731.3	1739.8	1746[h]
B3LYP	6-31G	1730.4	1748.0	
	6-31+G(*d*)	1812.6	1823.0	
	6-31+G(*d*,*p*)	1809.0	1819.5	

[a](C1-H3, C5-H7).
[b](C1-H4, C5-H8).
[c](O2 · · · H7, H3 · · · O6).
[d](O2-C1-H3, O6-C5-H7).
[e](O2-C1-H4, O6-C5-H8.
[f]Experimental harmonized wave numbers of fundamentals from ref. 24.
[g]Experimental harmonized wave numbers of fundamentals from ref. 25.
[h]Wave numbers of fundamental modes, see ref. 26.

harmonic frequencies for formaldehyde derived from the experimental information have been provided in the former articles.[24,25] Here, the predicted frequencies at MP2/6-311G(3*df*,2*p*), which are closer than the other basis sets, agree very well with the experimental vibrational spectrum. But the calculated values in Table 3 are unscaled. If one wants to compare with observed frequencies of fundamental modes, the scaling factor will be needed. To compare these four methods, we adopt the scaling factor for 6-31G(*d*) in ref. 43. After scaling the calculated frequency of C═O stretching mode by a factor of 0.994 for BLYP, the scaled wave numbers agree with the experimental values within 17 cm^{-1}. Scaling this mode by a factor of 0.961, B3LYP result is higher by 21 cm^{-1} while the frequencies of the remaining methods are about ±60 cm^{-1} than the experimental frequency.

Dimer

In the literature,[7,11–13] the general form of the angular planar geometry has been observed for the $H_2CO \cdots HX$ hydrogen-bonded complexes. In this section, the weak molecular complexes of the formaldehyde dimer are also observed in the similar form. In formaldehyde, the oxygen atom is the most nucleophilic region, and is conventionally pictured as carrying two lone pairs whose axes form with the C═O bond a trigonal planar arrangement about the oxygen atom. Thus, it predicts the planar equilibrium geometry for $H_2CO \cdots HX$, with an equilibrium C—O · · · H angle ∼120°.[7] For the dimer in this study such an equilibrium arrangement is with the angle about 108.7°.

Table 3 gives the ground-state equilibrium geometries of the formaldehyde dimer from DFT calculations with different basis sets. The structure of the cyclic formaldehyde dimer has a planar geometry with the two subunits bound through two nonlinear hydrogen bonds. One bond consists of the hydrogen atom (atom 3) of the left formaldehyde acting as the proton donor and the oxygen atom (atom 6) of the right formaldehyde acting as the acceptor while in the other the no. 7 formaldehyde proton interacts with the no. 2 oxygen atom. Table 3 also reports the harmonic vibrational frequency for the C═O stretching of formaldehyde dimer. Though IR investigations disclose no detailed information about the structures and energies of the dimer, theoretical studies are expected to reveal parameters of molecular geometries and predict their stabilities.

Oligomers $(H_2CO)_n$ (n = 3–7)

As we know, *ab initio* calculations can be extremely time consuming and vastly computational demanding. Otherwise, the DFT methods require significantly fewer computer resources. For these reasons, the calculated values are compared with corresponding

Table 4. Computed Geometries of Formaldehyde Oligomers by B3LYP/6-31+G(*d, p*).

	Bond lengths C—O (Å)	Bond angles ∠HCH (deg)	μ (D)	Energy SCF (a.u.)	Vibrational frequency
Experiment	1.208 (ref. 1)	116.5	2.33[e]		
	1.203 (ref. 4)	116.1	2.33[f]		
HCHO	1.209[a]	116.2[a]	2.51	−114.5115243	1819.5
$(HCHO)_2$	1.213[a,b]	117.3[a,b]	0.00	−229.0273539	1812.6
$(HCHO)_3$	1.213[a,c]	117.3[a,c]	2.45	−343.5427269	1807.1
	1.217[b]	118.2[b]			
$(HCHO)_4$	1.213[a,d]	117.3[a,d]	0.00	−458.0582668	1806.3
	1.217[b,c]	118.2[b,c]			
$(HCHO)_5$	1.213[a,c]	117.3[a,e]	2.44	−572.5736585	1805.7
	1.217[b,d]	118.3[b,d]			
	1.217[c]	118.3[c]			
$(HCHO)_6$	1.213[a,f]	117.3[a,f]	0.00	−687.0891699	1805.5
	1.217[b,e]	118.3[b,e]			
	1.217[c,d]	118.3[c,d]			
$(HCHO)_7$	1.213[a,g]	117.3[a,g]	2.44	−801.6045743	1805.4
	1.217[b,f]	118.2[b,f]			
	1.217[c,e]	118.3[c,e]			
	1.217[d]	118.3[d]			

[a](C1-O2); (H3-C1-H4).
[b](C5-O6); (H7-C5-H8).
[c](C9-O10); (H11-C9-H12).
[d](C13-O14); (H15-C13-H16).
[e](C17-O18); (H19-C17-H20).
[f](C21-O22); (H23-C21-H24).
[g](C25-O26); (H27-C25-H28).

experimental data. Finally, the B3LYP/6-31+G(*d*,*p*) is adapted for oligomers.

The geometries of formaldehyde oligomers are optimized by the B3LYP method using the 6-31+G(*d*,*p*) basis set. The molecular information of formaldehyde oligomers is tabulated in Table 4. The geometry of interacting molecules during complex formation influences determination of the intermolecular angles and distances. The calculations predict the lengthening of the C═O bond length upon complexation of dimer by 0.004 Å. The change of the C═O bond lengths upon trimer formation are elongated by 0.003 and 0.008 Å. For tetramer and so on, the predicted lengthening of C═O bond are elongated by 0.003 and 0.007 Å.

As we can see in Figure 1, individual formaldehyde in dimer offers one hydrogen atom to participate in the interaction. This characteristic agrees with the enlargement of the H—C—H bond angle by 1.1°. Next, we focus on the middle formaldehyde for trimer. The predicted H—C—H bond angles are, of course, larger than monomer and dimer. The two hydrogen atoms on the middle formaldehyde of trimer interact with the oxygen atoms of the side formaldehydes; thus, the H—C—H bond angle is 2.1° larger than that of the monomer. Furthermore, the H—C—H bond angle is 1.0° larger than the one of the dimer.

NLO Properties

Because the finite-field technique is a derivative method, the numerical problem cannot be avoided. To find out the values of the field strengths appropriate for the calculations of hyperpolarizabilities, some checks must be done on various oligomers for the numerical stability. Furthermore, the numerical accuracy of the finite-field equation is sensitive to the precision in the energy or the dipole moment calculation and also sensitive to the field strength. For these reasons, the suitable field strength for the calculations of the hyperpolarizability should be found out to prevent the numerical instability.

According to Lin[44] and Nakano et al.,[33–42] the calculations by the energy and dipole expressions do not give the same results. In addition, the results from the energy-based equation are more stable with respect to field strength, so only the energy-based equation has been chosen. Figures 2–5 show the variations of β_{zzz} and γ_{zzzz} of formaldehyde oligomers with field strengths by using the finite-field method and hyperpolarizability density analysis. As can be seen from these figures, one can find a numerically stable hyperpolarizability at a certain range of field strength, which is broader in FF than that in HDA. Consequently, the field strength of 0.013 a.u. is adopted to calculate the hyperpolarizabilities for all oligomers in FF while in the HDA approach, the field strength of 0.018 a.u. is chosen to plot hyperpolarizability densities.

Finite-Field Approach

Before addressing the analysis of the plots of HDA, it is necessary to make a few comments regarding our computational procedure compared to that used in previous work.[33,34] First, we use the standard basis set (6-31+G*) as the reference to compute the β_{zzz} by the Gaussian 98 program. Next, we compare the results calculated from the FF method using the stan-

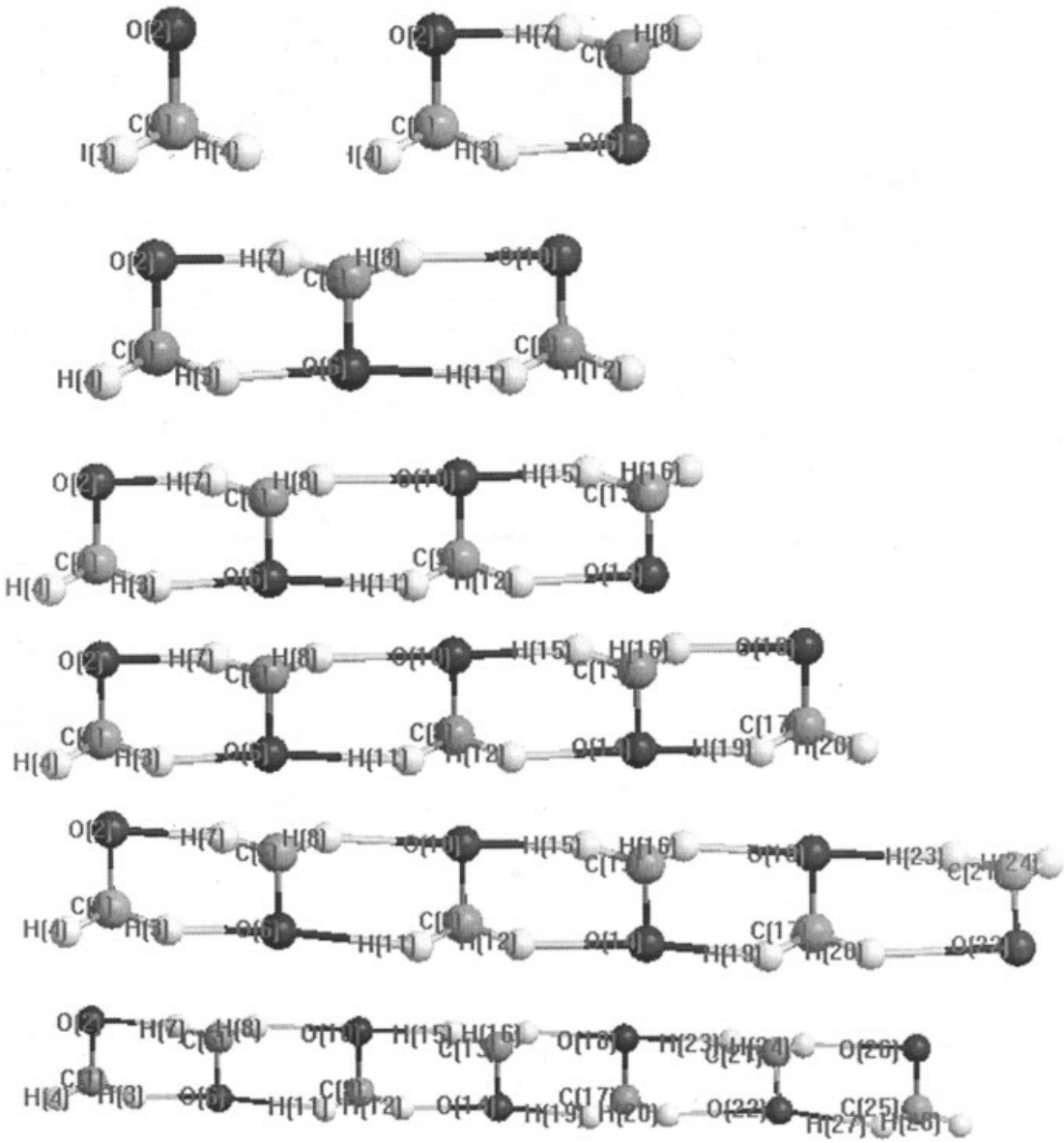

Figure 1. Formaldehyde oligomers.

dard basis sets (6-31+G* and 6-31++G**) and 6-31G + pd basis set with those from the G98 program. Figures 6 and 7 show the variations in the β_{zzz} and γ_{zzzz} respectively of H_2CO for various basis sets and electron correlation methods. The basis sets effects to γ_{zzzz} are greater than correlation effects. From the above discussion, we adopt the exponential Gaussian orbital parameters determined by Nakano et al.[33,34] for diffuse and polarization functions.

Basis Set Dependence of β_{zzz} and γ_{zzzz} for H_2CO

Although split-valence basis sets are found to yield variations of β_{zzz} and γ_{zzzz} with respect to electron correlation effects, the extended basis sets including both diffuse and polarization functions on the nonhydrogen atoms (6-31G + pd, 6-31G + pds, and 6-31G + pdsp) are found to be essential for obtaining sufficiently converged β_{zzz} and γ_{zzzz} of H_2CO in Nakano et al.'s report.[33,34] Figure 8 shows the variations in β_{zzz} of H_2CO for different basis sets and electron-correlation effects. This figure indicates that these basis sets can provide electron correlation dependence of β_{zzz} for H_2CO. The results obtained using these basis sets show that the augmentation of diffuse *s* function or/and polarization *p* function (6-31G + pds, 6-31G + pdp, and 6-31G + pdsp) on H atoms does not significantly affect the β_{zzz}. In addition, the triple split-valence basis set adding both diffuse *p* and polarization *d* functions (6-311G + pd) has a negligible effect on β_{zzz} in comparison with 6-31G + pd basis set.

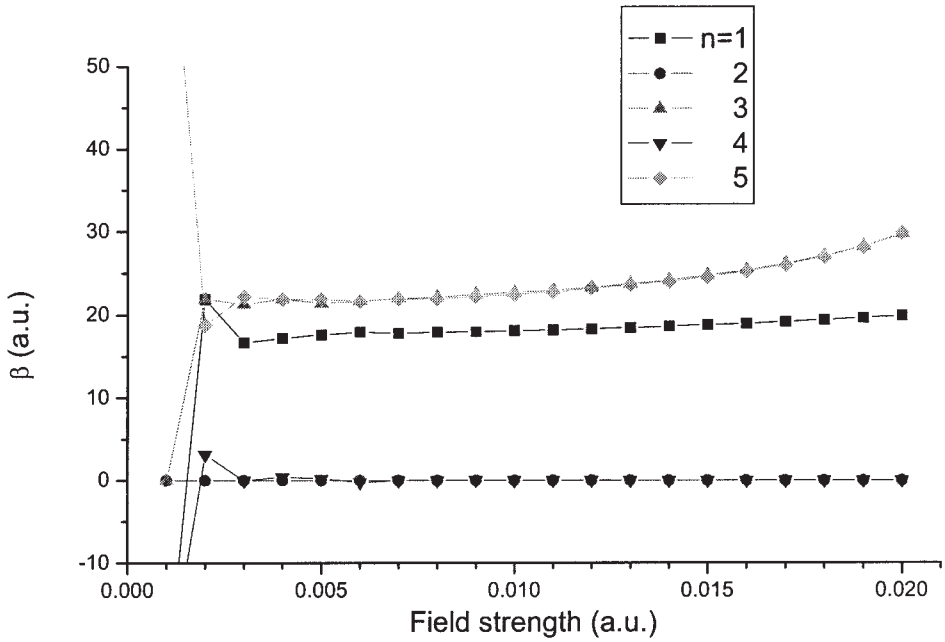

Figure 2. Variation of β_{zzz} with field strength for $(H_2CO)_n$ by finite-field method using B3LYP/6-31G + pd.

Figure 9 shows the variations in γ_{zzzz} of H_2CO for different basis sets and electron-correlation effects. This figure indicates that the basis sets in the absence of diffuse *p* and polarization *d* functions (6-31G) cannot provide a sufficient magnitude of γ_{zzzz} and an adequate description of the dependence of γ_{zzzz} on the electron correlation in contrast to the case of β_{zzz}. The results obtained using these basis sets show that the augmentation of the diffuse *s* function or/and the polarization *p* function (6-31G + pds, 6-31G + pdp, and 6-31G + pdsp) on H atoms does not significantly affect the γ_{zzzz}. In addition, the triple split-valence basis set adding both diffuse *p* and polarization *d* functions (6-311G + pd) has a negligible effect on γ_{zzzz} in comparison with 6-31G + pd basis set.

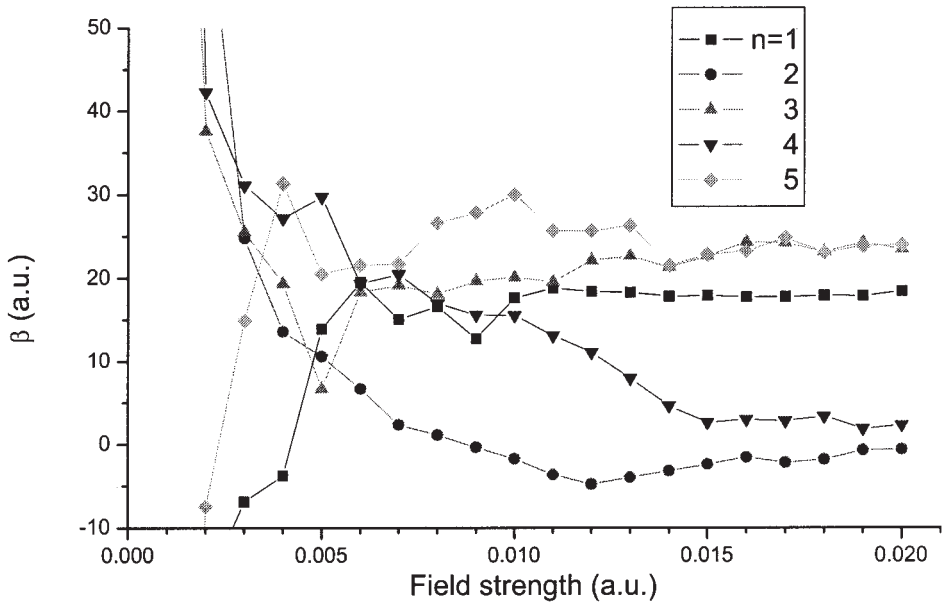

Figure 3. Variation of β_{zzz} with field strength for $(H_2CO)_n$ by hyperpolarizability density analysis using B3LYP/6-31G + pd.

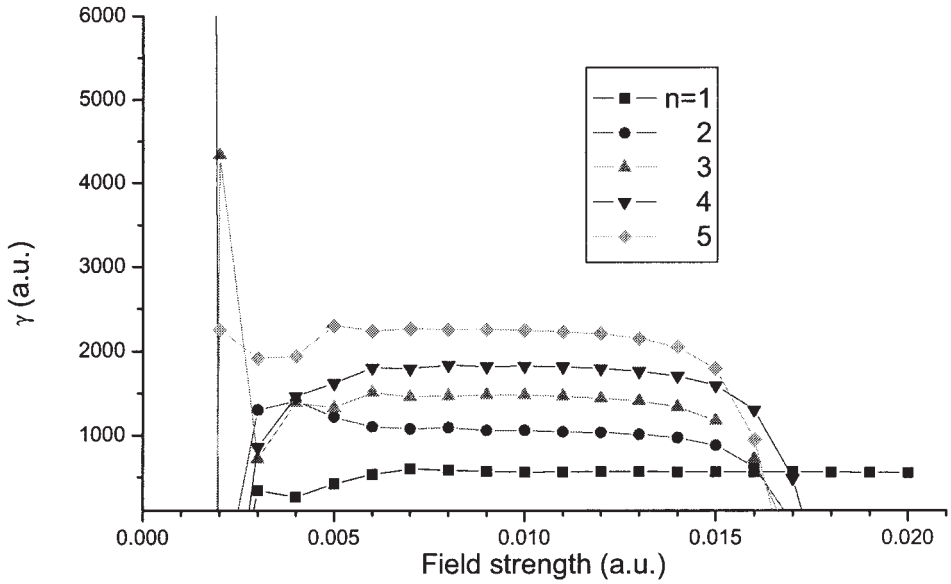

Figure 4. Variation of γ_{zzzz} with field strength for $(H_2CO)_n$ by finite-field method using B3LYP/6-31G + pd.

Electron Correlation Dependence of β_{zzz} and γ_{zzzz} for H_2CO

The β_{zzz} and γ_{zzzz} values calculated by using the 6-31G + pd basis set are used in the following discussion concerning the electron correlation dependence of β_{zzz} and γ_{zzzz}. As shown in Figure 8, there are remarkable differences in the magnitude and electron correlation dependences of β_{zzz} for H_2CO calculated by the 6-31G + pd basis set. In particular, the correlation effects by the MP2 method decrease the β_{zzz} of H_2CO at the HF level. The correlation effects by the MP3 method are found to slightly decrease β_{zzz} from the MP2 value. In the MP4 computations, the effects of *S* and *T* excitations provide positive contributions to β_{zzz}. A comparison between the CCD and MP4DQ for β_{zzz} suggests that the correlation effects originating from higher order *D* excitations beyond the fourth-order are negligible. The β_{zzz} calculated by the CCSD method is considerably larger than that by the CCD method. These results indicate that the correlation corrections originating from higher order *S* excitations are essential

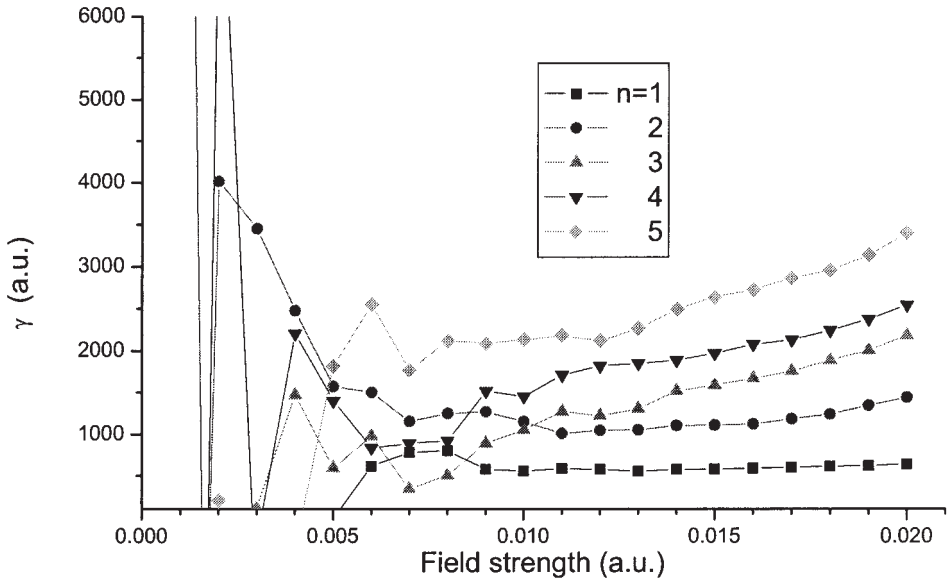

Figure 5. Variation of γ_{zzzz} with field strength for $(H_2CO)_n$ by hyperpolarizability density analysis using B3LYP/6-31G + pd.

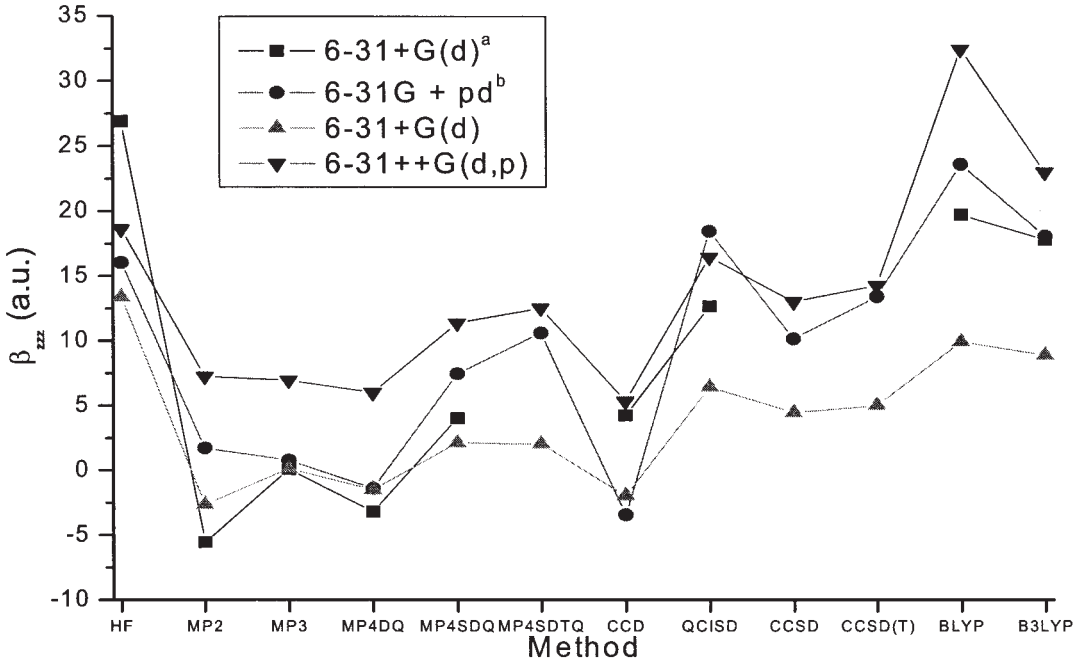

Figure 6. Variations in the β_{zzz} of H_2CO for various basis sets and electron correlation methods. ([a]Standard basis set. [b]Exponential Gaussian orbital parameters determined by Nakano et al.)

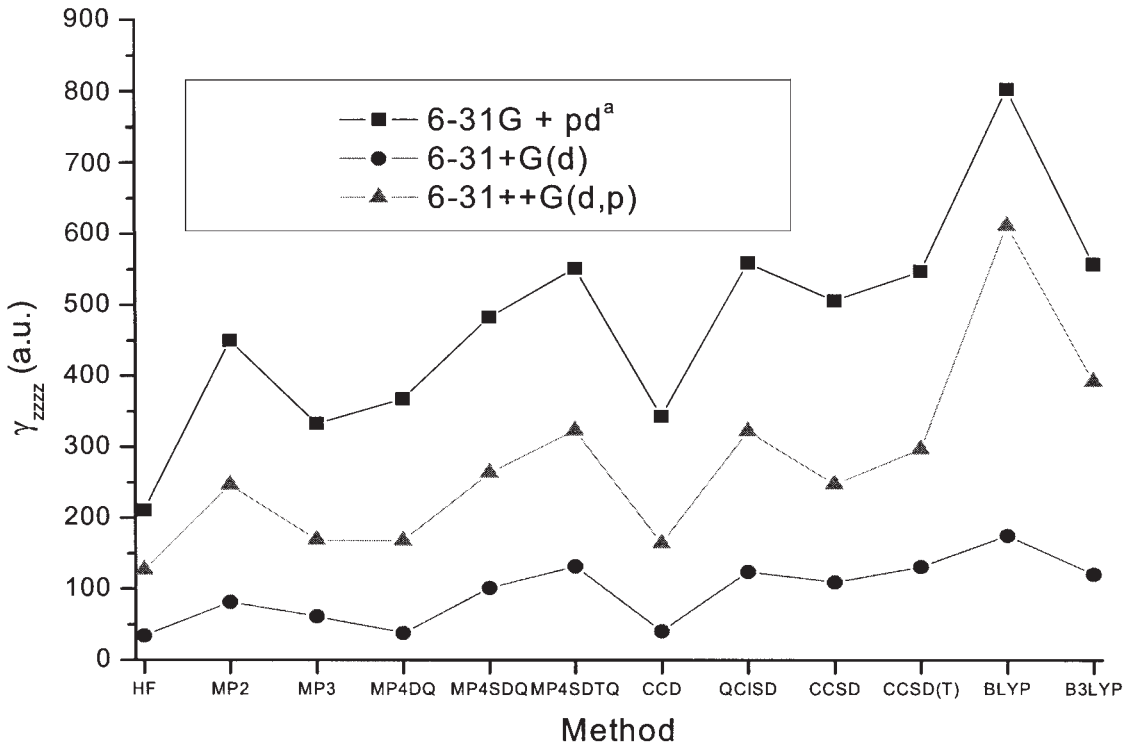

Figure 7. Variations in the γ_{zzzz} of H_2CO for various basis sets and electron correlation methods. ([a]Exponential Gaussian orbital parameters determined by Nakano et al.)

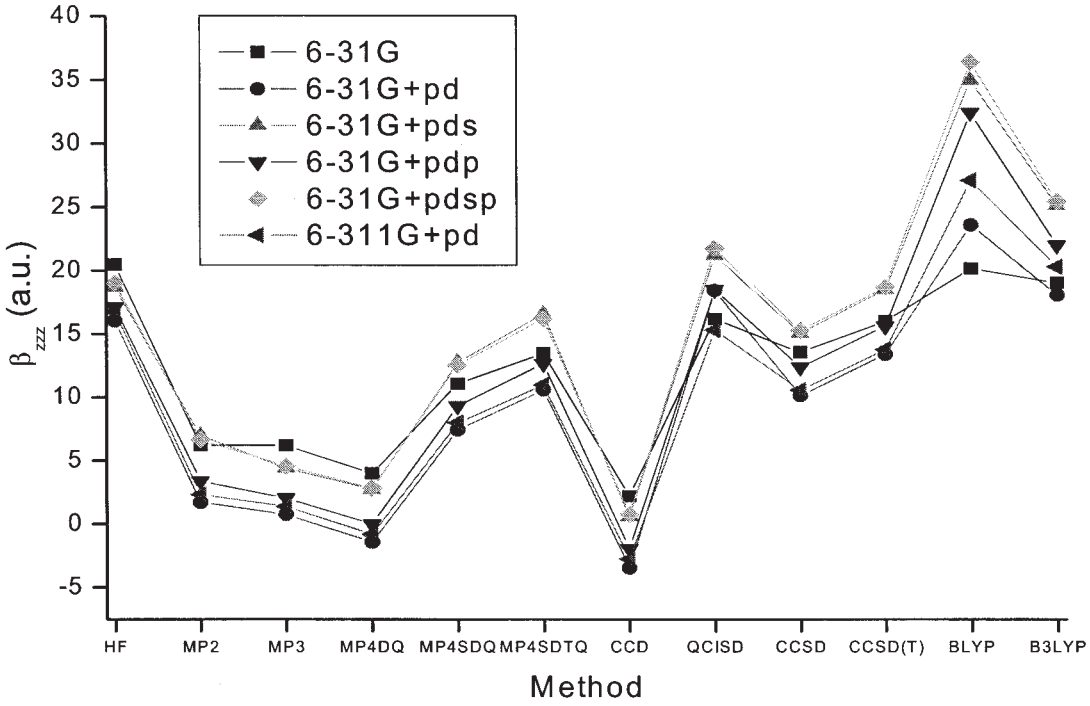

Figure 8. Variations in the β_{zzz} of H_2CO for various basis sets and electron correlation methods using field strength of 0.01 a.u.

for evaluating the β_{zzz} quantitatively. In addition, the β_{zzz} calculated by the CCSD method and by the MP4SDQ method are nearly equal; therefore, it is clear that the higher order correlation effects caused by *S* and *D* excitations beyond the fourth-order contribute only a little to the β_{zzz}. The QCISD method can reproduce the β_{zzz} of H_2CO by the CCSD method. Further, the β_{zzz} by the CCSD(T)

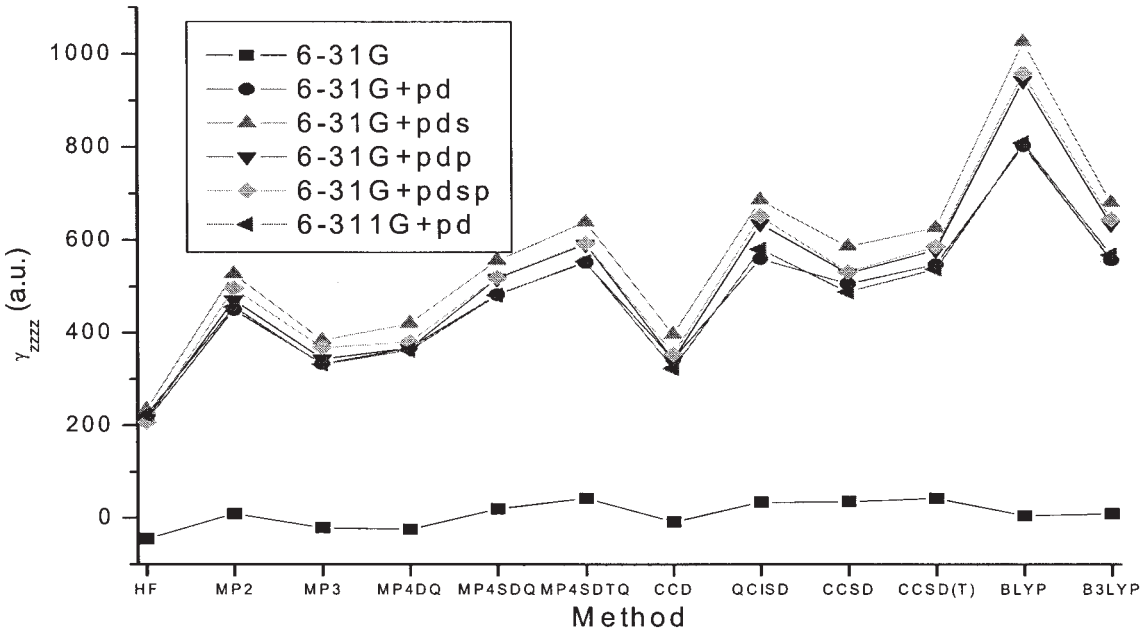

Figure 9. Variations in the γ_{zzzz} of H_2CO for various basis sets and electron correlation methods using field strength of 0.01 a.u.

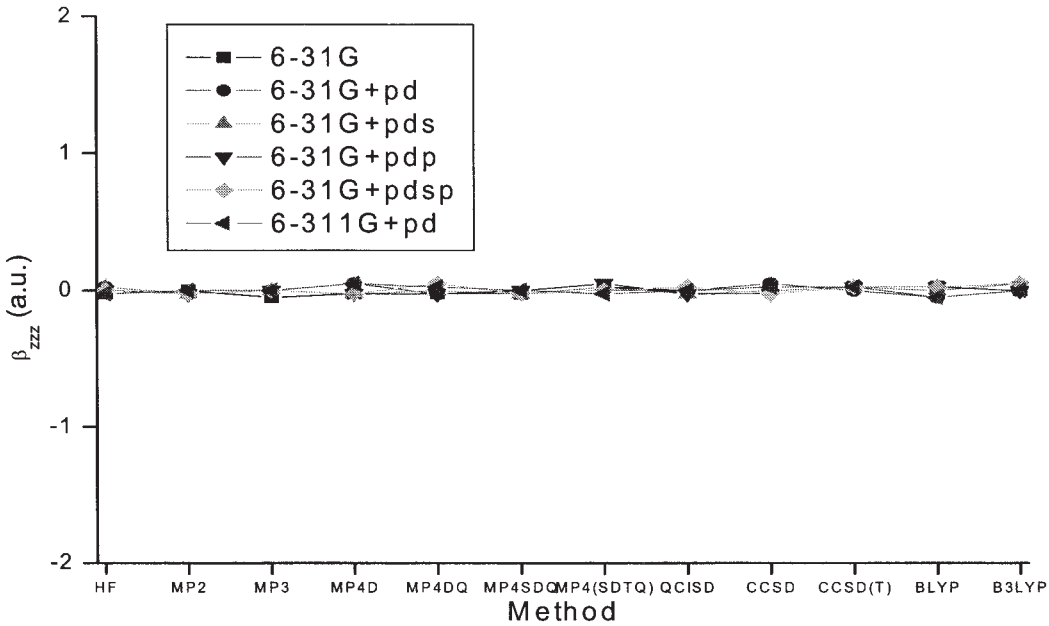

Figure 10. Variations in the β_{zzz} of $(H_2CO)_2$ for various basis sets and electron correlation methods using field strength of 0.01 a.u.

method are shown to be nearly equal to those by the CCSD method. As judged from the magnitudes and signs of β_{zzz}, the CCSD(T), CCSD, QCISD, and MP4SDTQ methods are found to provide nearly converged β_{zzz}. The β_{zzz} by BLYP method are larger than those by the CCSD(T) method. But B3LYP can satisfactorily reproduce the β_{zzz} of H_2CO by the CCSD(T) method.

The γ_{zzzz} calculated by the MP2 method is shown to be close to the γ_{zzzz} calculated by the CCSD method. As shown in Figure 9, there are remarkable differences in the magnitude and electron correlation dependences of γ_{zzzz} for H_2CO calculated by 6-31G + pd basis set. In particular, the correlation effects by the MP2 method decrease the β_{zzz}, but greatly increase the γ_{zzzz} of H_2CO

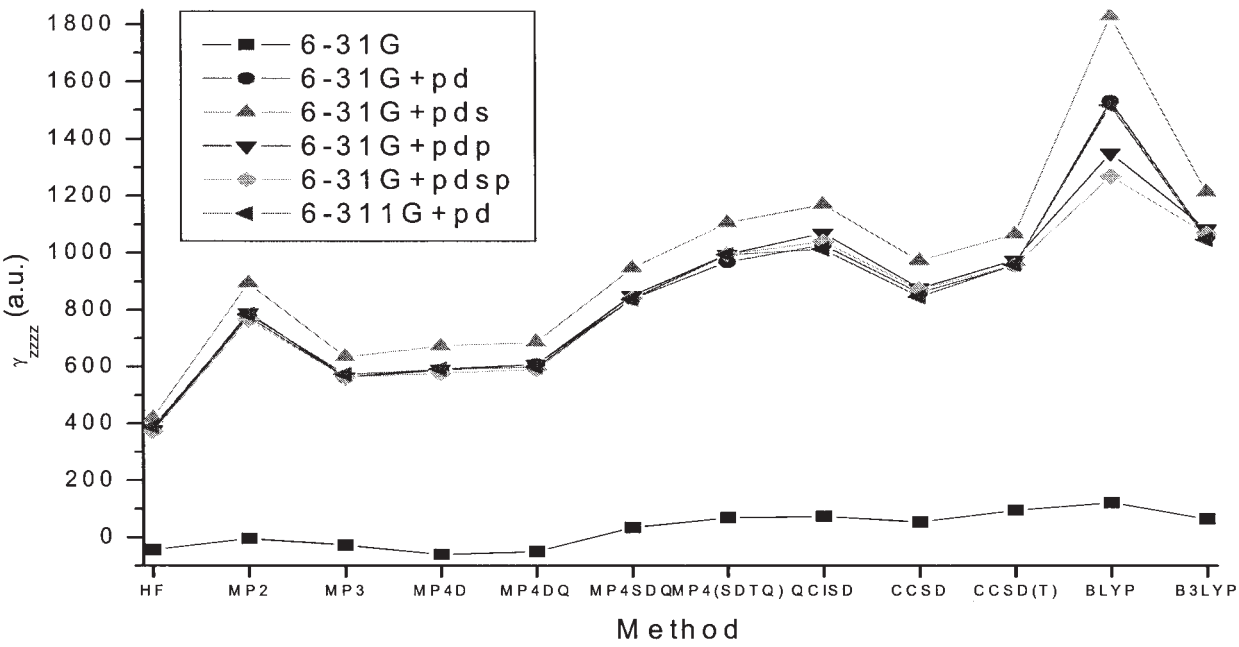

Figure 11. Variations in the γ_{zzzz} of $(H_2CO)_2$ for various basis sets and electron correlation methods using field strength of 0.01 a.u.

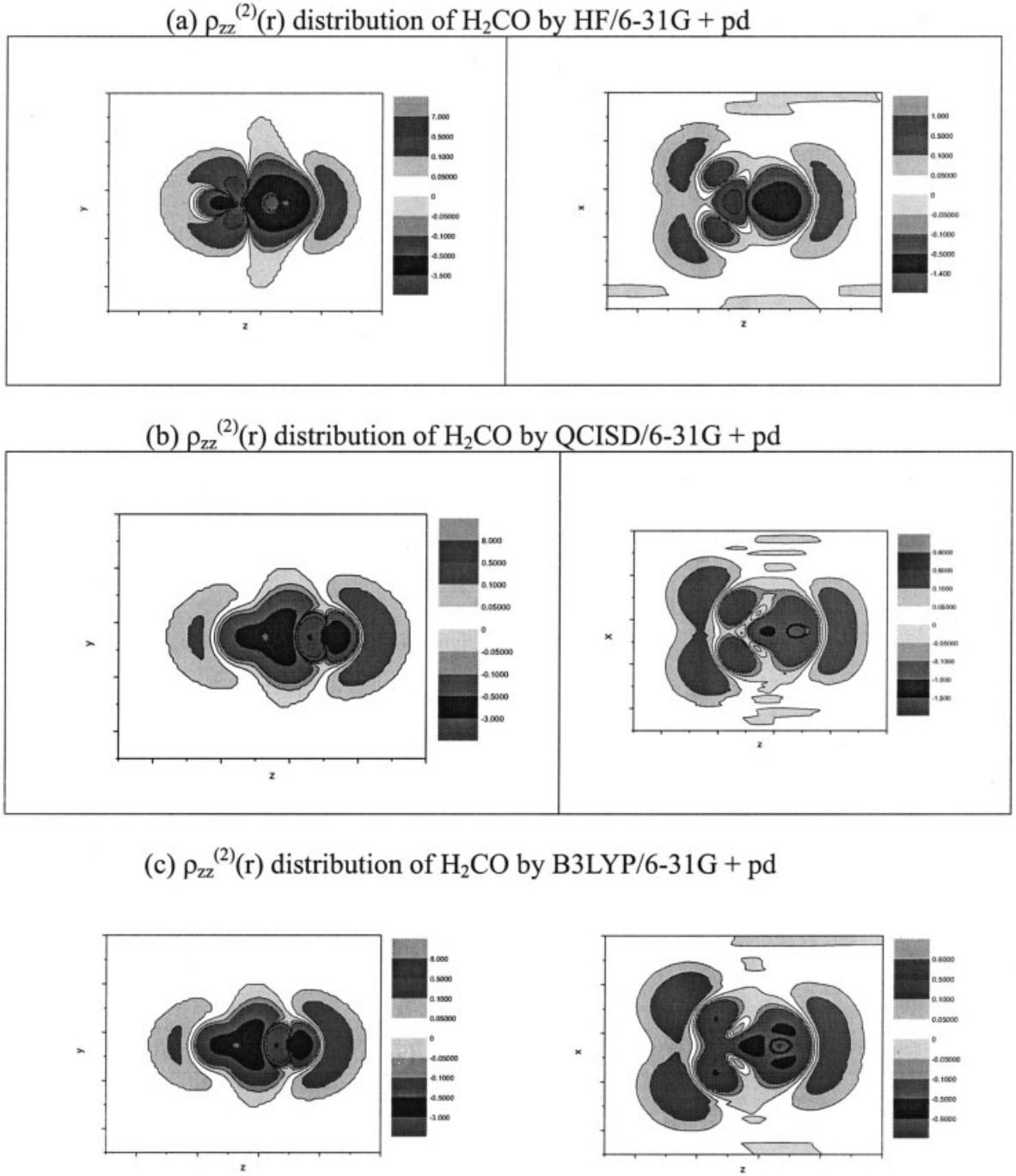

Figure 12. Contour plots of β_{zzz} densities on the σ_v and σ_v' + 1.0 a.u. planes of H_2CO.

at the HF level. The correlation effects by the MP3 method are found to decrease γ_{zzzz} from the MP2 value. In the MP4 computations, the effects of *S* and *T* excitations provide positive contributions to γ_{zzzz}. A comparison between the CCD and MP4DQ for γ_{zzzz} suggests that the correlation effects originating from higher order *D* excitations beyond the fourth-order are negligible. The γ_{zzzz} calculated by the CCSD method is considerably larger than that by the CCD method. These results indicate that the correlation corrections originating from higher order *S* excitations are essential for evaluating the γ_{zzzz} quantitatively. In addition, the γ_{zzzz} calculated by the CCSD method and by the MP4SDQ method are nearly equal; therefore, it is clear that the higher order correlation effects caused by *S* and *D* excitations beyond the fourth-order contribute only a little to the γ_{zzzz}. The QCISD method can

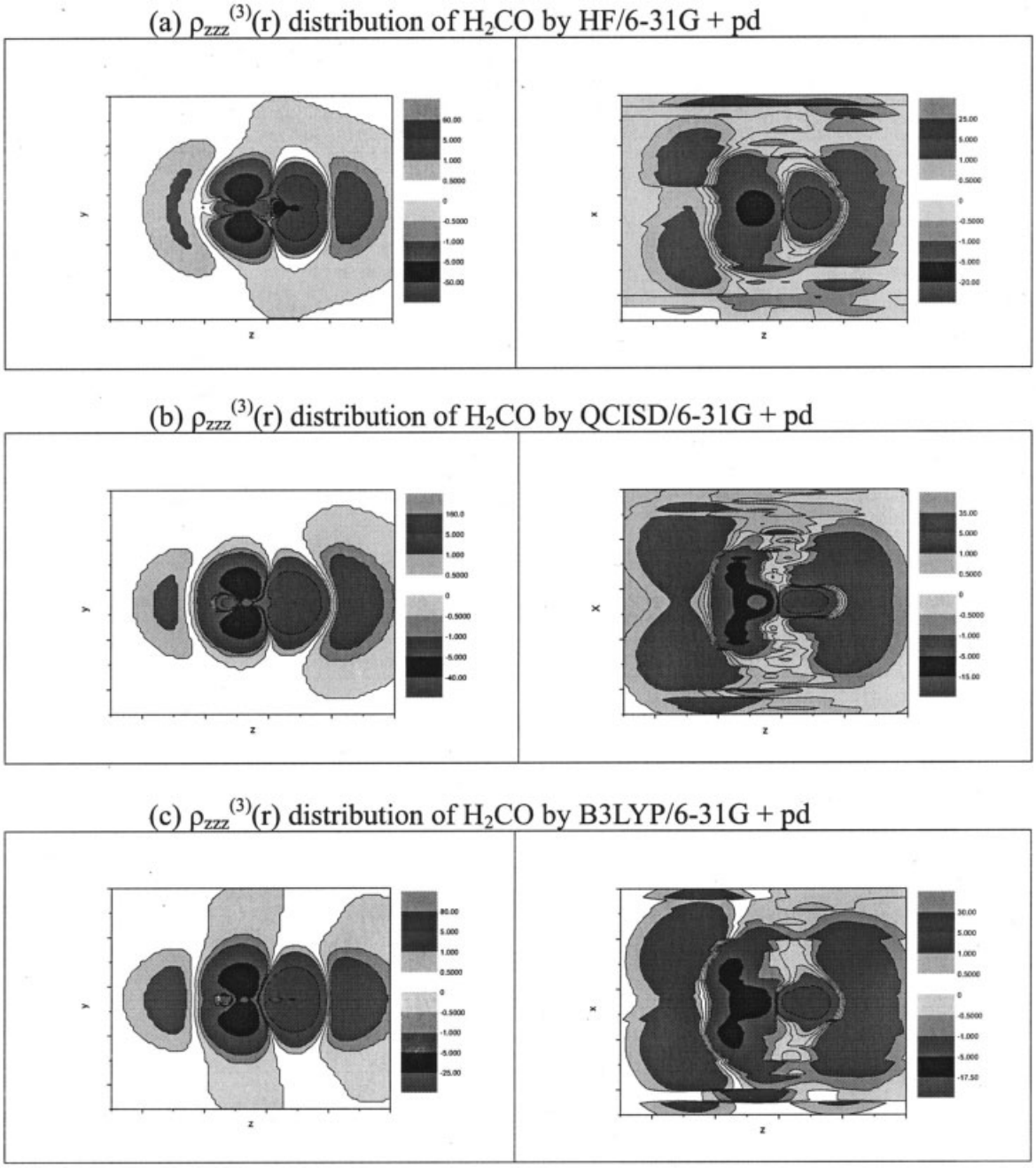

Figure 13. Contour plots of γ_{zzzz} densities on the σ_v and σ_v' + 1.0 a.u. planes of H_2CO.

reproduce the γ_{zzzz} of H_2CO by the CCSD method. Further, the γ_{zzzz} by the CCSD(T) method are shown to be nearly equal to those by the CCSD method. As judged from the magnitudes and signs of γ_{zzzz}, for obtaining converged γ_{zzzz} the CCSD(T), CCSD, QCISD, MP4SDTQ, as well as MP4SDQ methods seem to be essential, and they can be qualitatively reproduced by the MP2 method. The γ_{zzzz} by BLYP method are larger than those by the CCSD(T) method. But B3LYP can satisfactorily reproduce the γ_{zzzz} of H_2CO by the CCSD(T) method.

Basis Set Dependence of β_{zzzz} and γ_{zzzz} for the Dimer

Because the $(H_2CO)_2$ is centrosymmetry, the value of β_{zzz} for this species is zero. As can be seen in Figure 10, the basis set dependence of β_{zzz} for $(H_2CO)_2$ is negligible. Figure 11 shows the variations in γ_{zzzz} of $(H_2CO)_2$ for different basis sets and electron-correlation effects. This figure indicates that the basis sets in the absence of diffuse p and polarization d functions (6-31G) cannot provide a sufficient magnitude of γ_{zzzz} and an adequate description

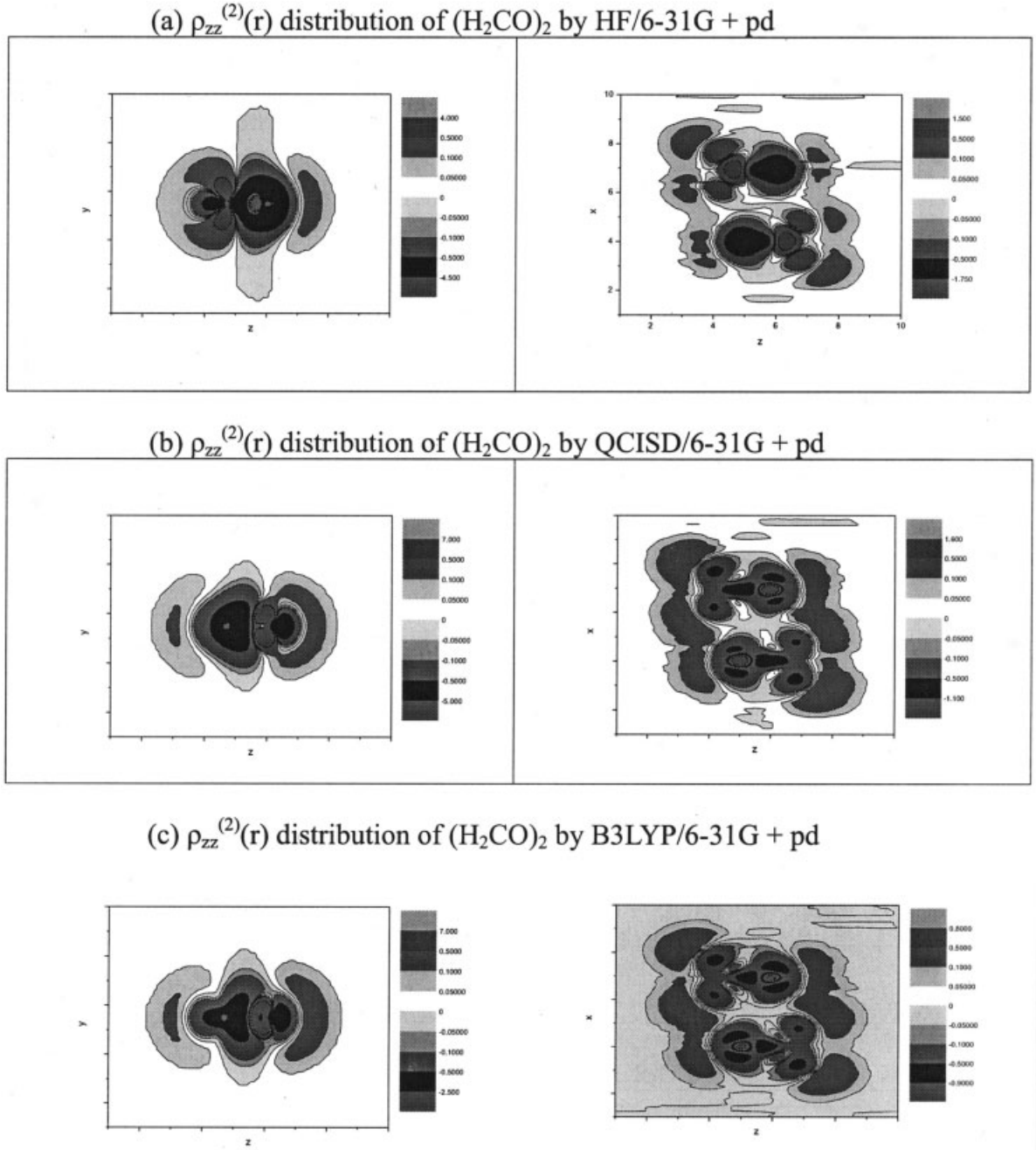

Figure 14. Contour plots of β_{zzz} densities on the σ_v and σ_v' + 1.0 a.u. planes of $(H_2CO)_2$.

of the dependence of γ_{zzzz} on the electron correlation similar to the case of γ_{zzzz} for H_2CO. The results obtained using these basis sets show that the augmentation of polarization *p* function and/or diffuse *s* function (6-31G + pdp, and 6-31G + pdsp) on *H* atoms does not significantly affect the γ_{zzzz} except for the BLYP values. For the effect of the diffuse *s* function (6-31G + pds), the values of the variations in γ_{zzzz} of $(H_2CO)_2$ for electron correlation methods are overestimated. In addition, the triple split-valence basis set adding both diffuse *p* and polarization *d* functions (6-311G + pd) has a negligible effect on γ_{zzzz} in comparison with 6-31G + pd basis set.

Electron Correlation Dependence of β_{zzz} and γ_{zzzz} for the Dimer

As shown in Figure 10, the magnitude and electron correlation dependences of β_{zzz} for the dimer calculated by different basis sets are almost the same. Figure 11 reports the variations in the γ_{zzzz},

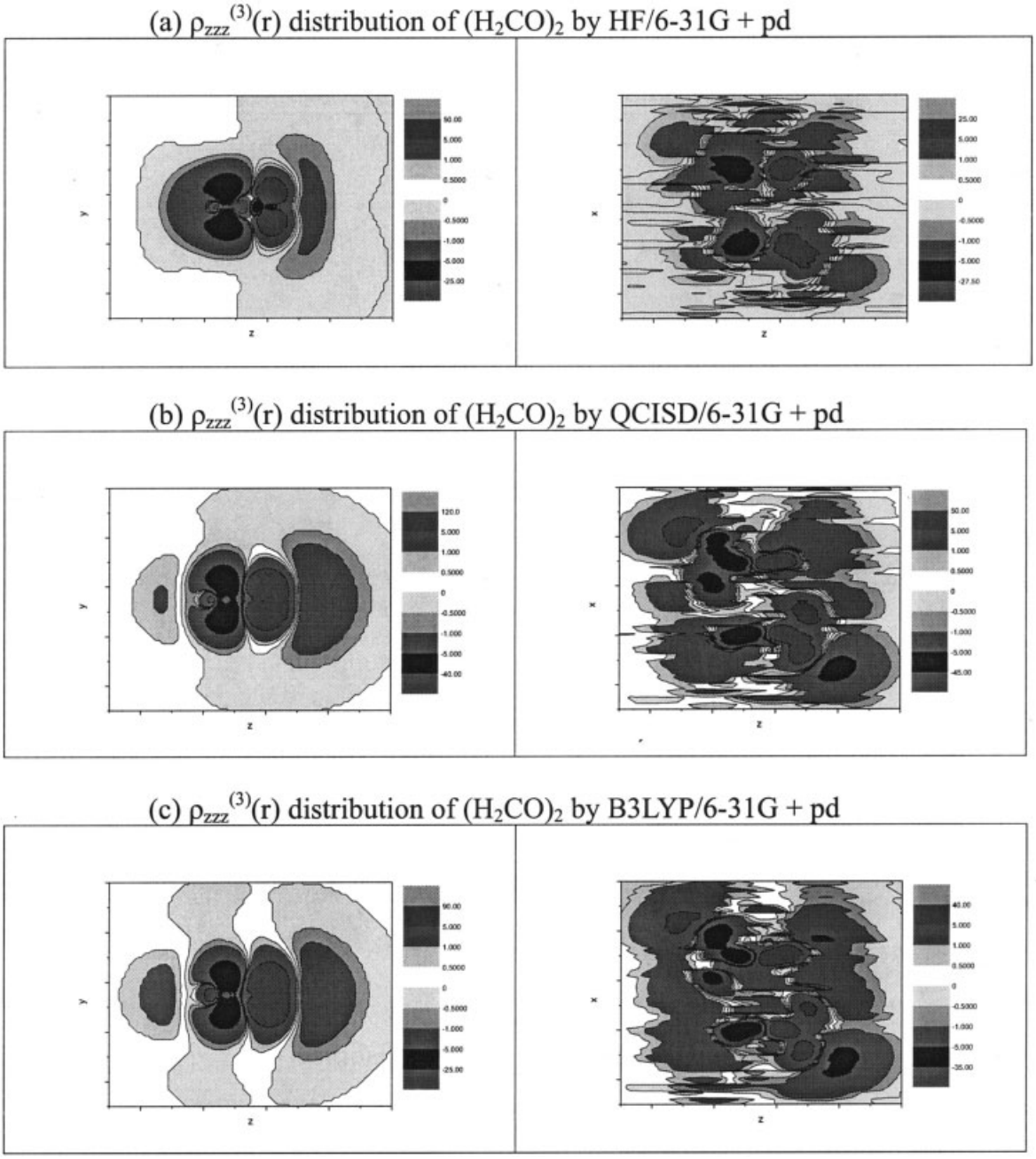

Figure 15. Contour plots of γ_{zzzz} densities on the σ_v and σ_v' + 1.0 a.u. planes of $(H_2CO)_2$.

for which the tendency of the electron correlation effects is similar to that for the formaldehyde monomer. There are remarkable differences in the magnitude and electron correlation dependences of γ_{zzzz} for $(H_2CO)_2$. In particular, the correlation effects by the MP2 method greatly increase the γ_{zzzz} of $(H_2CO)_2$ at the HF level. The correlation effects by the MP3 method are found to decrease γ_{zzzz} from the MP2 value. In the MP4 computations, the effects of *S* and *T* excitations increase the γ_{zzzz} values for $(H_2CO)_2$. A comparison between the CCSD and MP4SDQ for γ_{zzzz} suggests that the correlation effects originating from higher order *S* and *D* excitations beyond the fourth-order are negligible. The γ_{zzzz} calculated by the CCSD(T) method is slightly larger than that by the CCSD method. These results indicate that the correlation corrections originating from higher order *T* excitations are essential for evaluating the γ_{zzzz} quantitatively. In addition, the γ_{zzzz} calculated by the CCSD(T) method and by the MP4(SDTQ) method are nearly equal; therefore, it is clear that the higher order correlation effects caused by *S*, *D*, and *T* excitations beyond the fourth-order

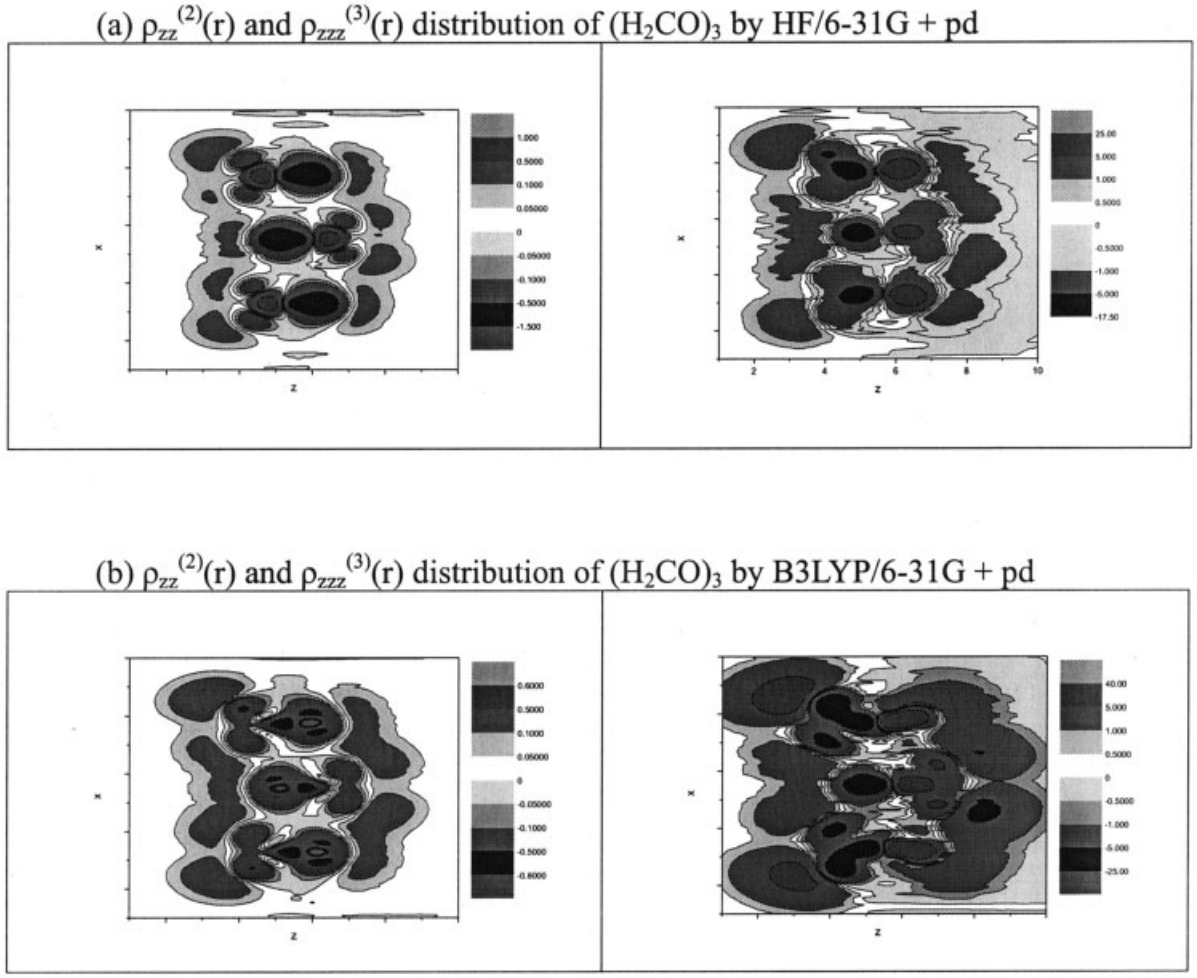

Figure 16. Contour plots of β_{zzz} and γ_{zzzz} densities on the σ_v' + 1.0 a.u. planes of $(H_2CO)_3$.

contribute only a little to the γ_{zzzz} for $(H_2CO)_2$. Further, the QCISD method can reproduce the γ_{zzzz} of $(H_2CO)_2$ by the CCSD(T) method. As judged from the magnitudes and signs of γ_{zzzz}, the CCSD(T), QCISD, and MP4(SDTQ) methods are found to provide nearly converged γ_{zzzz}, and they can be qualitatively reproduced by the MP2 method. As we can see in Figure 11, the γ_{zzzz} of $(H_2CO)_2$ by the B3LYP method is shown to be nearly equal to those by the QCISD method. Compared with the CCSD(T) method, the γ_{zzzz} of $(H_2CO)_2$ by B3LYP method is about 10% larger than those by this method.

From Figures 8–11, the B3LYP method can reproduce the hyperpolarizabilities of H_2CO monomer and dimer by QCISD method. Therefore, on the one hand, we used the QCISD method to see the difference between these two methods (B3LYP and QCISD) in hyperpolarizability density analysis, and on the other, we used the HF method to see the electron correlation effects. In summary of the basis sets and electron correlation effects, the β_{zzz} and γ_{zzzz} calculated by B3LYP using the 6-31G + pd basis set are used in the following discussion where the HF method is used for comparison.

Hyperpolarizability Density Analysis

This analysis can illustrate qualitative differences in the spatial contributions of electrons to hyperpolarizabilities. Because we focus on the contribution of π electrons to the β_{zzz} and γ_{zzzz}, the plane at which the β_{zzz} and γ_{zzzz} densities drawn is located at 1.0 a.u. above the molecular plane.

Spatial Contributions to β_{zzz} and γ_{zzzz} for Formaldehyde

To characterize the electron correlation effects, we first investigate the spatial contributions to β_{zzz} and γ_{zzzz} by using plots of $\rho_{zz}^{(2)}(r)$ and $\rho_{zzz}^{(3)}(r)$. From Nakano et al.'s results, we can see that a correct description of the spatial characteristics of the contour of $\rho_{zz}^{(2)}(r)$ and $\rho_{zzz}^{(3)}(r)$ for H_2CO requires the inclusion of higher order S excitation effects. According to the above results and the discussion, we choose the HF, QCISD, and B3LYP methods using the 6-31G + pd basis set to plot the pictures of hyperpolarizability density. Figures 12 and 13 give contour plots of $\rho_{zz}^{(2)}(r)$ and $\rho_{zzz}^{(3)}(r)$

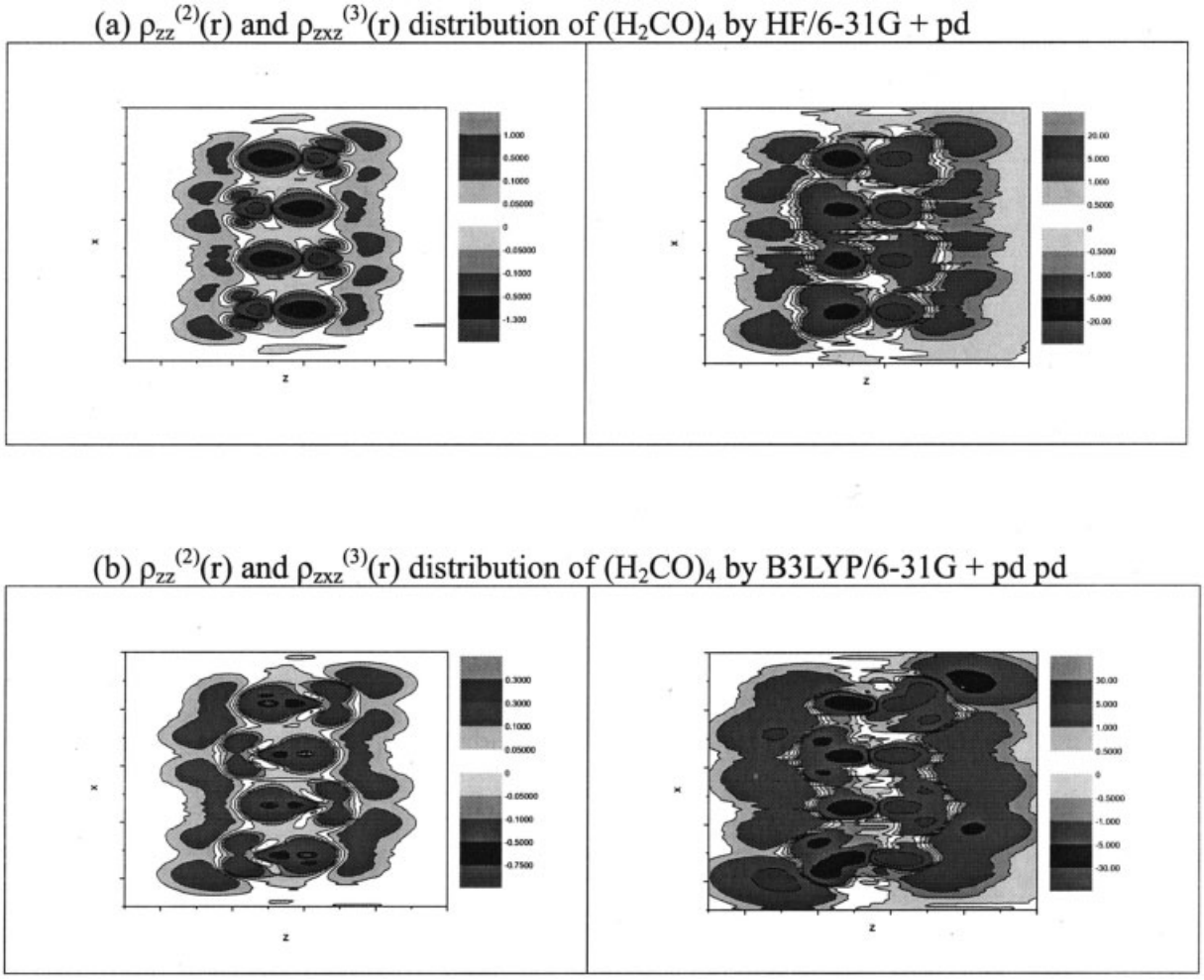

Figure 17. Contour plots of β_{zzz} and γ_{zzzz} densities on the σ_v' + 1.0 a.u. planes of $(H_2CO)_4$.

on the σ_v planes (yz-planes) and σ_v' + 1.0 a.u. planes (xz-planes) of H_2CO, respectively.

In the plots of $\rho_{zz}^{(2)}(r)$ by the HF method, Nakano et al.[33,34] showed that diffuse p and d functions slightly enlarge the regions of the π-electron contributions to the β_{zzz} at HF/6-31G. These features support the small basis set dependences of β_{zzz} shown in Figure 8. For β_{zzz} at the HF level, the π-electron regions contribute to β_{zzz} positively, in contrast to the σ-electron regions (in the direction of the C═O bond axis), which make negative contributions to β_{zzz}. Because π electrons provide the main contributions, the total β_{zzz} for H_2CO at the HF level becomes slightly positive.

A comparison among the plots of $\rho_{zz}^{(2)}(r)$ for H_2CO at 6-31G + pd in Figure 12a–c shows that the spatial contributions from the outer π-electron regions (xz-planes) are enlarged by the electron correlation effect. It is also observed that the contour plots of $\rho_{zz}^{(2)}(r)$ for H_2CO at QCISD/6-31G + pd are similar to that at B3LYP/6-31G + pd. Therefore, the B3LYP/6-31G + pd method can provide the correct tendency of β_{zzz} including sufficient electron correlation effects for this closed-shell system.

In the plots of $\rho_{zzz}^{(3)}(r)$ by the HF method, Nakano et al.[39,40] showed that diffuse p and d functions create two outer regions on both sides of the main regions of $\rho_{zzz}^{(3)}(r)$ at HF/6-31G. These features agree with the variations in γ_{zzzz} of H_2CO for basis set effects (Fig. 9). The outer π electrons contribute to γ_{zzzz} positively, contrary to the internal π-electron regions, which make negative contributions to γ_{zzzz}, giving positive contributions to the total γ_{zzzz}. For the γ_{zzzz} at HF/6-31G,[39] however, the $\rho_{zzz}^{(3)}(r)$ of π electrons provides negative contributions to the total γ_{zzzz}.

A comparison among the plots of $\rho_{zz}^{(3)}(r)$ for H_2CO at 6-31G + pd shows that the spatial contributions from the outer π-electron regions (xz-planes) are enlarged by the electron correlation effect. It can also be seen that the contour plots of $\rho_{zzz}^{(3)}(r)$ for H_2CO at QCISD/6-31G + pd are similar to that at B3LYP/6-31G + pd. Therefore, the B3LYP/6-31G + pd method can provide the correct

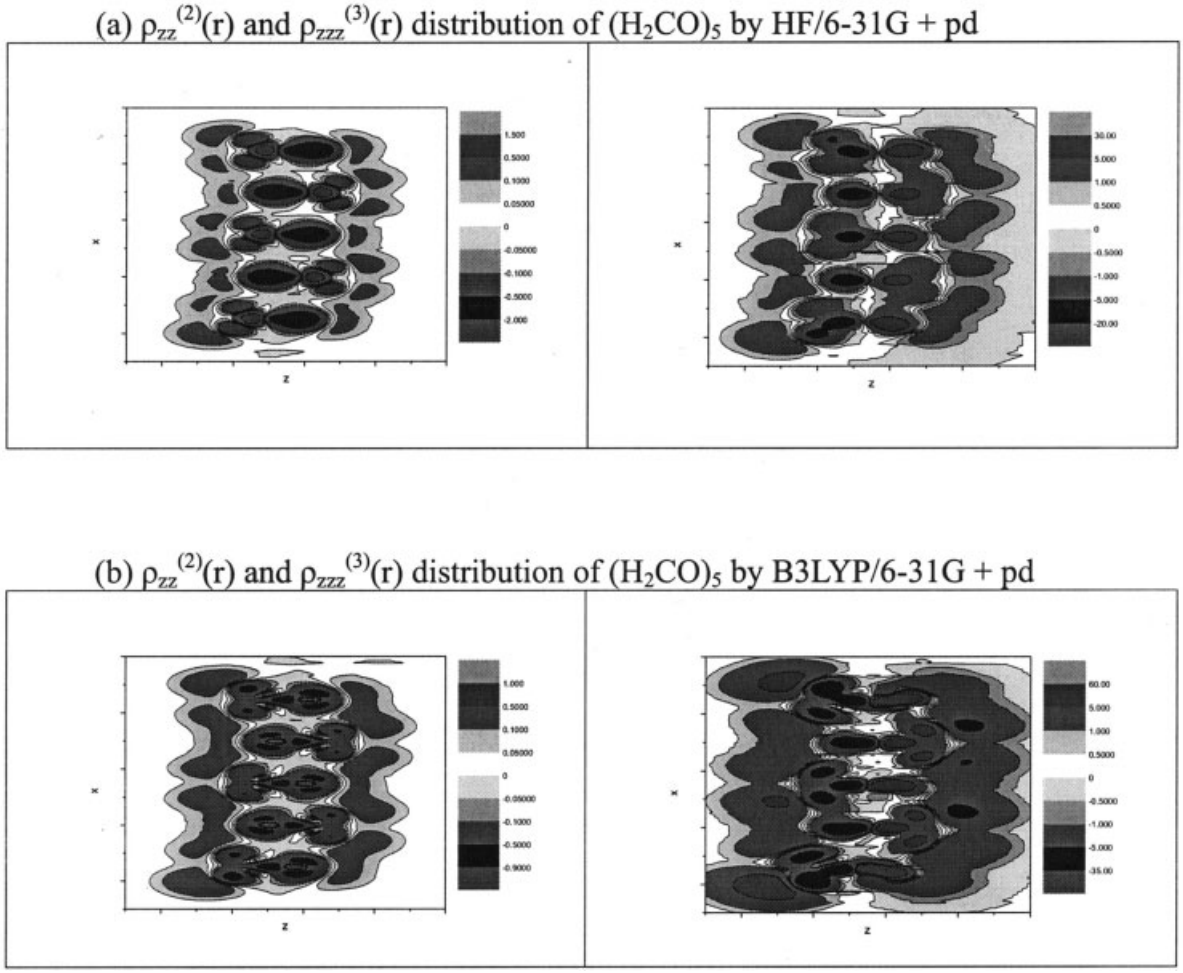

Figure 18. Contour plots of β_{zzz} and γ_{zzzz} densities on the σ_v' + 1.0 a.u. planes of $(H_2CO)_5$.

tendency of γ_{zzzz} including sufficient electron correlation effects for this closed-shell system.

Spatial Contributions to β_{zzz} and γ_{zzzz} for Formaldehyde Dimers

Figure 14 gives contour plots of $\rho_{zz}^{(2)}(r)$ on the σ_v planes (yz-planes, the formaldehyde molecule in the dimer) and the σ_v' + 1.0 a.u. planes (xz-planes) of the dimer as well as Figure 15 is for the γ_{zzzz} density plots.

The σ_v planes show the hyperpolarizability density distributions of σ-electron regions are much similar to that of H_2CO monomer. For the contour plots of β_{zzz} density distributions on the plane located at 1.0 a.u. above the plane of the dimer, we can see the middle parts are the dominant density distribution regions, which exhibit the cancel effect to the β_{zzz} and make the β_{zzz} value equal to zero. So the small electron correlation dependences of β_{zzz} support the variations in Figure 10. From this dimer we can see the contour plot of each formaldehyde molecule has the same shape and magnitude. In addition, it is also much similar to the monomer.

The outer γ_{zzzz} density distribution regions in the xz-plane at the QCISD and B3LYP levels are shown to increase compared with that at the HF level, contrary to the internal regions. As can be seen from the γ_{zzzz} density distributions of the formaldehyde dimer at these levels, two main outer regions in the xz-plane contribute to γ_{zzzz} positively, in contrast to the internal regions, which make negative contributes to γ_{zzzz}. Therefore, it is clear to see that the total γ_{zzzz} value for the H_2CO dimer at the HF level represents less positively than the others.

For the contour plots of $\rho_{zz}^{(2)}(r)$ or $\rho_{zzz}^{(3)}(r)$, the shapes and signs for the upper part and the lower one in the opposite positions are the same. On the other hand, the $\rho_{zzz}^{(3)}(r)$ values are very different from $\rho_{zz}^{(2)}(r)$. Although the contour plots have the same shape in opposite direction, the difference is the hyperpolarizability density distributions have inverse values.

Compared with the xz-plane of H_2CO, it is found that the intermolecular interaction between the hydrogen atom of one molecule and the oxygen atom of the other can be clearly figured out in the interaction regions. The weak interactions do not contribute to the β_{zzz}. In the contour plots of $\rho_{zzz}^{(3)}(r)$, the interaction

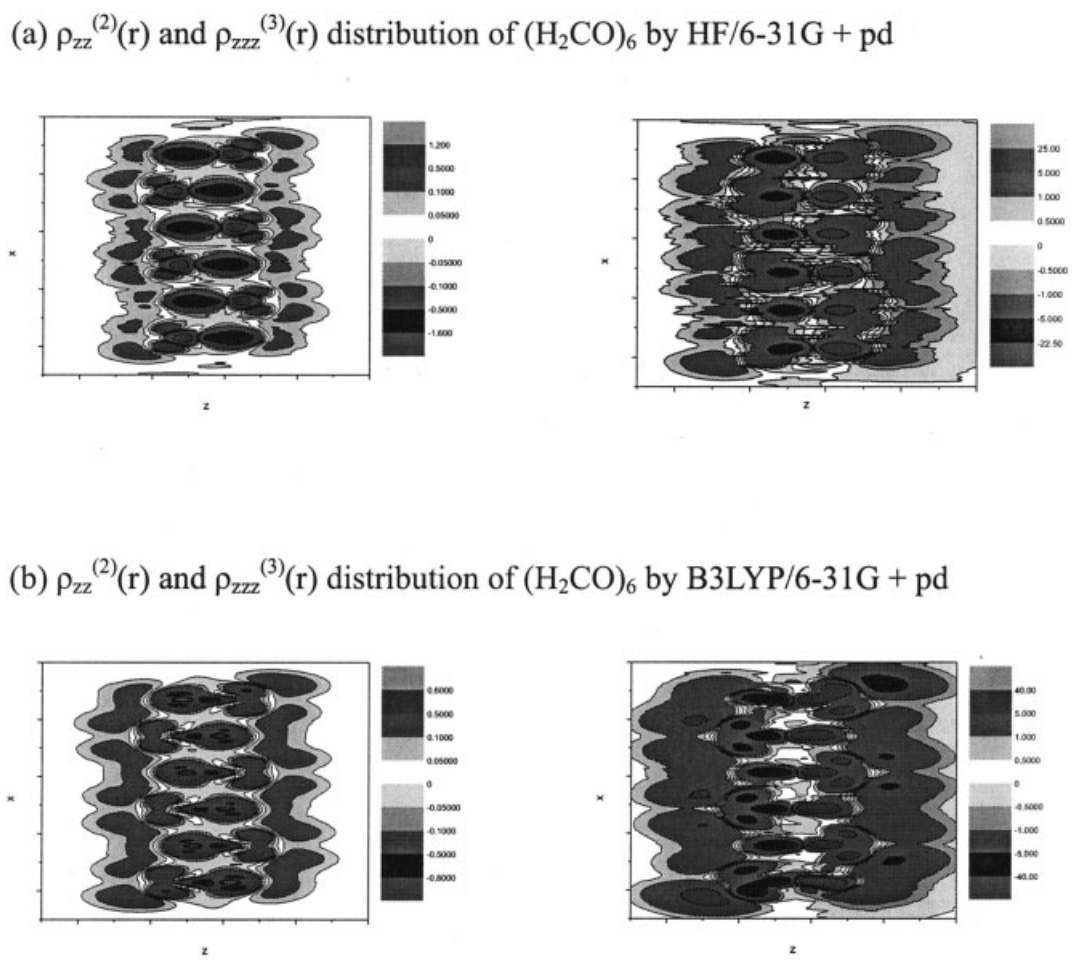

Figure 19. Contour plots of β_{zzz} and γ_{zzzz} densities on the σ_v' + 1.0 a.u. planes of $(H_2CO)_6$.

regions at the main outer regions also contribute to γ_{zzzz} positively. It is also noted that in the β_{zzz}, the γ_{zzzz} values and their density distributions obtained by using QCISD and B3LYP methods well coincide with each other in the signs, magnitude, and shapes of the distributions.

Spatial Contributions to β_{zzz} and γ_{zzzz} for Formaldehyde Oligomers

Examination of the formaldehyde oligomers $(H_2CO)_n$, concerning the pictures on the σ_v' + 1.0 a.u. planes (xz-planes), clearly shows that when going from the monomer to the formaldehyde dimer or similarly from the dimer to the formaldehyde oligomers $(H_2CO)_{3-7}$ we can find some of the features of the initial species. This gives a local view of spatial contributions of electrons to the β_{zzz} and γ_{zzzz}. In addition, it is also interesting to notice that around the atoms in the opposite positions, the contour maps behave in a similar fashion, that is, the same sequencing of positive and negative regions for β_{zzz} in contrast to γ_{zzzz}. Furthermore, we notice that a common feature emerging from the contour plots is the large contributions (positive and negative) in the outer regions to the second electronic hyperpolarizability.

In this first comparison, that is, dimer vs. trimer, it may be seen that the cancel effects are presented in the figures of β_{zzz} density distributions, so the total contributions represent the β_{zzz} values of trimer near the monomer. Next, we can clearly see that the outer γ_{zzzz} density distribution regions in the xz-plane at the HF and B3LYP levels are shown to be enlarged compared with the dimer. Because these major regions increase, the numerical values of γ_{zzzz} increase. When comparing the methods, we can find the increasing outer regions at B3LYP method are larger than that at the HF level.

Here again, examining the $(H_2CO)_4$ maps reveal that the β_{zzz} is responsible for the internal β_{zzz} density distribution regions. Similar to the dimer, the numerical value of β_{zzz} of $(H_2CO)_4$ is vanishing. The situation is different for the second hyperpolarizability. Compared with the dimer, the γ_{zzzz} value is increasing, as reflected in the contour plots, which are almost two times the size of the dimer. According to the above comparison, the hyperpolarizability density distributions of $(H_2CO)_{5-7}$ like $(H_2CO)_{1-2}$ have similar contributions.

In the above discussion, it may be observed graphically that the hyperpolarizability density distributions on the plane located at

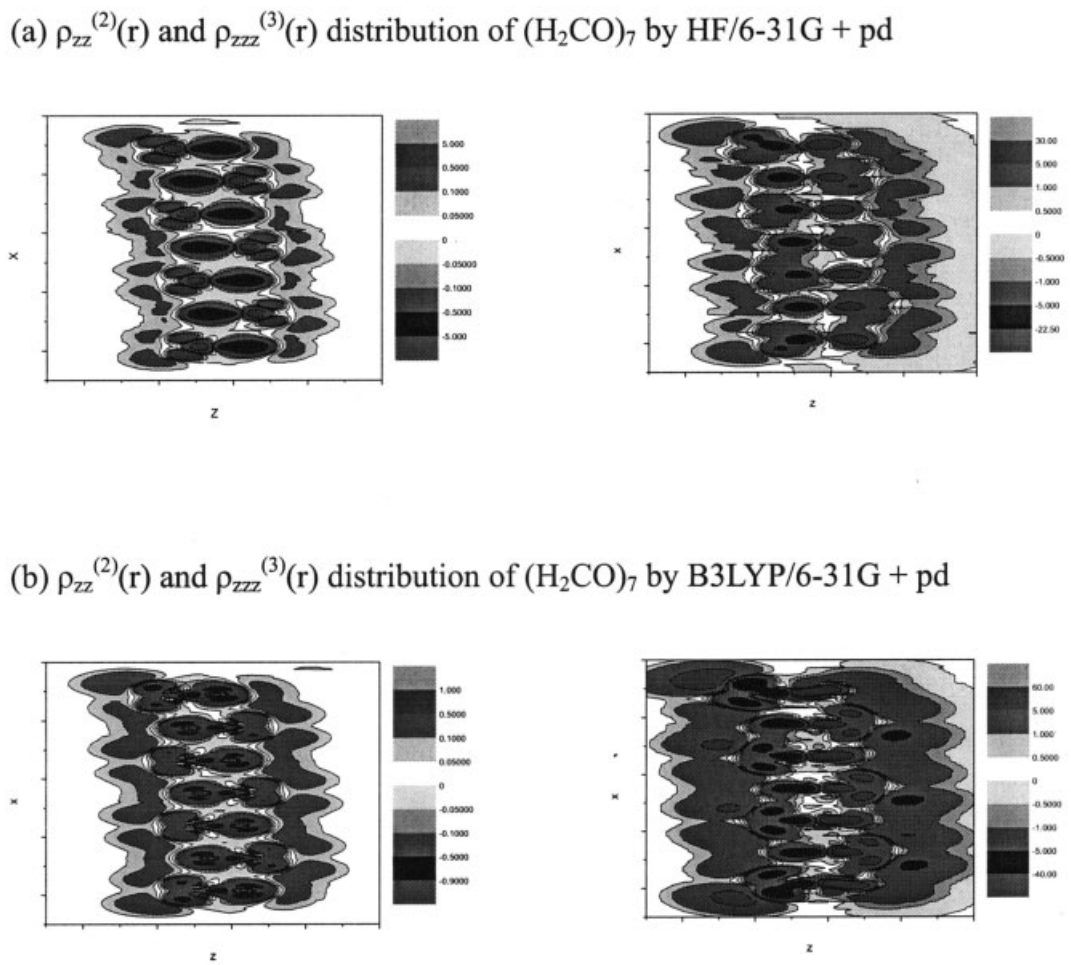

Figure 20. Contour plots of β_{zzz} and γ_{zzzz} densities on the σ_v' + 1.0 a.u. planes of $(H_2CO)_7$.

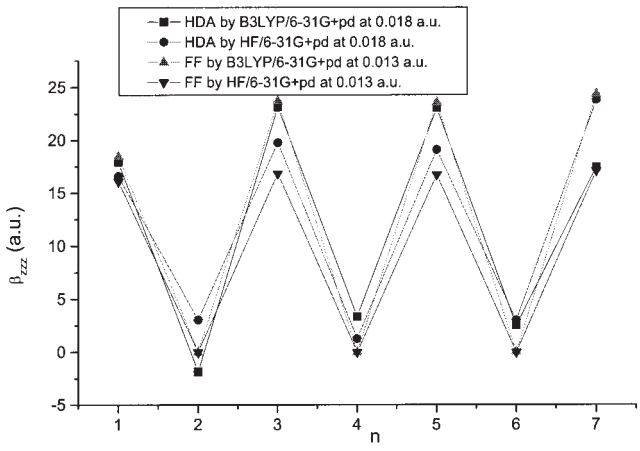

Figure 21. β_{zzz} of H_2CO oligomers $(H_2CO)_n$ using the HF and B3LYP methods.

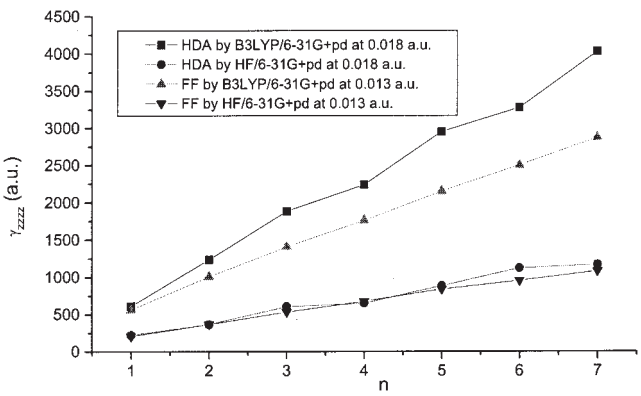

Figure 22. γ_{zzzz} of H_2CO oligomers $(H_2CO)_n$ using the HF and B3LYP methods.

1.0 a.u. above the plane of the formaldehyde oligomers are proportional to the hyperpolarizabilities values. More precisely, the contour plots of $\rho^{(2)}_{zz}(r)$ and $\rho^{(3)}_{zzz}(r)$ of $(H_2CO)_{3-7}$ at the HF and B3LYP levels are similar to those of the monomer and dimer. As a consequence of this, the following presents a summary of some observations from comparing the monomer and $(H_2CO)_{2-7}$:

1. In the computational level, the hyperpolarizability density distributions of formaldehyde oligomers can be qualitatively reproduced by the HF method, but the magnitude of the NLO responses is smaller than those by the B3LYP method.
2. In β_{zzz}, the internal distribution regions are the main contributions. In this region, we can clearly see that how the cancel effects affect the first hyperpolarizability.
3. In γ_{zzzz}, the major contributions are the outer γ density distribution regions, and the internal counterparts are minor contributions. The main contributions are positive but the internal regions contribute to γ_{zzzz} negatively. To sum these regions, it provides positive contributions to the γ_{zzzz}.

Variations of the β_{zzz} and γ_{zzzz} of Formaldehyde Oligomers for the FF and HDA Approaches

For the sake of completeness, the calculated values for β_{zzz} and γ_{zzzz} of $(H_2CO)_{1-7}$ are given in Figures 21 and 22, respectively. At the HF level, the difference in the hyperpolarizability computational approaches is small. However, the difference for B3LYP level is increasing with n. Thus, the following presents a summary of some observations from comparing the monomer and $(H_2CO)_{2-7}$:

1. In β_{zzz}, when n is even, the value is zero because the molecule possesses centrosymmetry. But when n is odd, the differences among the numerical values of β_{zzz} are not clear.
2. In γ_{zzzz}, the value of γ_{zzzz} increases with n.

Conclusions

This work examined the possibility of using a pictorial approach to understand how the longitudinal hyperpolarizabilities result from local contributions distributed over space. The following conclusions can be drawn from the results of the present study of the formaldehyde oligomers $(H_2CO)_n$:

1. For the formaldehyde monomer (H_2CO), the geometries given by MP2/6-311G(3*df*,2*p*) and B3LYP/6-31+G(*d*,*p*) are in good agreement with the experimental data. For formaldehyde oligomers, all atoms lie on the same plane (*xz*-plane).
2. For $(H_2CO)_{1-2}$ calculated by the FF and HDA methods, the B3LYP method can reproduce the hyperpolarizabilities and the contour plots of hyperpolarizabilities density at the QCISD level.
3. For the dimer, the features of longitudinal γ can be analyzed by partitioning the π-electron contribution into regions. It is found that the outer region mainly contributes to the γ_{zzzz} positively and the contribution of the internal region is smaller negatively.
4. From the numerical stability checking of the hyperpolarizability calculations, the calculated values by the FF method are more stable than those by the HDA approach. The present HDA method seems inadequate, as intermolecular interaction is taken into account.
5. In β_{zzz}, when n is even, the value is zero because the molecule possesses centrosymmetry. When n is odd, the differences among β_{zzz} are not clear. For the value of γ_{zzzz}, it increases with n. It is furthermore noticed that in the case of the hyperpolarizabilities, the principle of additivity can be applied in the first hyperpolarizability.

References

1. Shen, Y. R. The Principles of Nonlinear Optics; Wiley: New York, 1986.
2. Maiman, T. H. Nature 1960, 187, 493.
3. Prasad, P. N.; Williams, D. J. Introduction to the Nonlinear Optical Effects in Molecules and Polymers; Wiley: New York, 1991.
4. Williams, D. J., Ed. Nonlinear Optical Properties of Organic and Polymeric Materials; ACS Symposium Series 233; Americal Chemical Society: Washington, DC, 1983.
5. Messier, J.; Kajar, F.; Prasad, P. N., Eds. Organic Molecules for Nonlinear Optics and Photonics; Kluwer Scientific Publishers: Dordrecht, 1991.
6. Walker, J. F. Formaldehyde; Reinhold Publishing Corporation: New York, 1944.
7. Howard, N. W.; Legon, A. C. J Chem Phys 1988, 88, 6793.
8. Rice, J. E.; Amos, R. D.; Colwell, S. M.; Handy, N. C.; Sanz, J. J Chem Phys 1990, 93, 8828.
9. Deng, L.; Ziegler, T.; Fan, L. J Chem Phys 1993, 99, 3823.
10. Wilkie, J.; Williams, I. H. J Chem Soc Perkin Trans 1995, 2, 1559.
11. Pecul, M.; Leszczński, J.; Sadlej, J. J Chem Phys 2000, 112, 7930.
12. Branchadell, V.; Oliva, A. J Am Chem Soc 1991, 113, 4132.
13. Nowek, A.; Leszczński, J. J Chem Phys 1996, 104, 1441.
14. Yang, H.; Liau, Y.-H.; Su, T.-M. J Phys Chem 1995, 99, 177.
15. Versluis, L.; Ziegler, T. J Chem Phys 1988, 88, 322.
16. Kwiatkowski, J. S.; Leszczynski, J. Mol Phys 1994, 81, 119.
17. Harris, N. J. J Phys Chem 1995, 99, 14689.
18. Kwiatkowski, J. S.; Leszczynski, J. Int J Quantum Chem 1992, 26, 421.
19. Kwiatkowski, J. S.; Leszczynski, J. J Mol Spectrosc 1993, 157, 540.
20. Martin, J. M. L. Chem Phys Lett 1995, 242, 343.
21. Carter, S.; Handy, N. C.; Demaison, J. Mol Phys 1997, 90, 729.
22. Carter, S.; Pinnavaia, N.; Handy, N. C. J Chem Phys 1995, 240, 400.
23. Duncan, J. L. Mol Phys 1974, 28, 1177.
24. Wohar, M. M.; Jagodzinski, P. W. J Mol Spectrosc 1991, 148, 13.
25. Harding, L. B.; Ermler, W. C. J Comput Chem 1985, 6, 13.
26. Majoube, M.; Derreumaux, P.; Vergoten, G. XII Int Conf of Raman Spectr 1990, 150.
27. Kondo, K.; Oka, T. J Phys Soc Jpn 1960, 109, 9674.
28. Fabricant, B.; Krieger, D.; Mautner, J. S. J Chem Phys 1977, 67, 1576.
29. Matthews, P. S. C. Quantum Chemistry of Atoms and Molecules; Cambridge University Press: London, 1986.
30. Frisch, M. J.; Trucks, G. W.; Schlegel, H. B.; Scuseria, G. E.; Robb, M. A.; Cheeseman, J. R.; Zakrzewski, V. G.; Montgomery, J. A., Jr.; Stratmann, R. E.; Burant, J. C.; Dapprich, S.; Millam, J. M.; Daniels, A. D.; Kudin, K. N.; Strain, M. C.; Farkas, O.; Tomasi, J.; Barone, V.; Cossi, M.; Cammi, R.; Mennucci, B.; Pomelli, C.; Adamo, C.; Clifford, S.; Ochterski, J.; Petersson, G. A.; Ayala, P. Y.; Cui, Q.; Morokuma, K.; Malick, D. K.; Rabuck, A. D.; Raghavachari, K.; Foresman, J. B.; Cioslowski, J.; Ortiz, J. V.; Stefanov, B. B.; Liu, G.; Liashenko,

A.; Piskorz, P.; Komaromi, I.; Gomperts, R.; Martin, R. L.; Fox, D. J.; Keith, T.; Al-Laham, M. A.; Peng, C. Y.; Nakayakkara, A.; Gonzalez, C.; Challacombe, M.; Gill, P. M. W.; Johnson, B. G.; Chen, W.; Wong, M. W.; Andres, J. L.; Head–Gordon, M.; Replogle, E. S.; Pople, J. A. Gaussian 98, Rev. A.6; Gaussian, Inc.: Pittsburgh, PA, 1998.
31. Nakano, M.; Yamaguchi, K. Chem Phys Lett 1993, 206, 285.
32. Nakano, M.; Shigemoto, I.; Yamada, S.; Yamaguchi, K. J Chem Phys 1995, 103, 4175.
33. Yamada, S.; Nakano, M.; Shigemoto, I.; Yamaguchi, K. Chem Phys Lett 1996, 254, 158.
34. Yamada, S.; Nakano, M.; Shigemoto, I.; Kiribayashi, S.; Yamaguchi, K. Chem Phys Lett 1997, 267, 445.
35. Yamada, S.; Nakano, M.; Yamaguchi, K. Chem Phys Lett 1997, 276, 375.
36. Nakano, M.; Yamada, S.; Yamaguchi, K. Chem Phys Lett 1999, 306, 187.
37. Nakano, M.; Yamada, S.; Yamaguchi, K. Chem Phys Lett 1999, 311, 221.
38. Nakano, M.; Yamada, S.; Yamaguchi, K. J Phys Chem 1999, 103, 3103.
39. Yamada, S.; Nakano, M.; Yamaguchi, K. J Phys Chem 1999, 103, 7105.
40. Nakano, M.; Yamada, S.; Yamaguchi, K. Chem Phys Lett 2000, 321, 491.
41. Nakano, M.; Fujita, H.; Takahata, M.; Yamaguchi, K. J Chem Phys 2001, 115, 1052.
42. Nakano, M.; Fujita, H.; Takahata, M.; Yamaguchi, K. J Chem Phys 2001, 115, 6780.
43. Scott, A. P.; Radom, L. J Phys Chem 1996, 100, 16502.
44. Lin, Y.-T. Computational Studies of Structural Effects on Nonlinear Optical Responses of Some π-Conjugated Molecules; Master's Thesis, National Chung Cheng University: Taiwan, 1996.